AD-A033 891 KENTUCKY UNIV LEXINGTON DEPT OF ENGINEERING MECHANICS F/G 12/1
THE BOUNDARY INTEGRAL EQUATION METHOD USING VARIOUS APPROXIMATI--ETC(U)
DEC 76 Y S WU
AF-AFOSR-2824-75
UNCLASSIFIED AFOSR-TR-76-1313 NL

1 OF 2
AD A033891

12

THE BOUNDARY INTEGRAL EQUATION METHOD USING VARIOUS APPROXIMATION TECHNIQUES FOR PROBLEMS GOVERNED BY LAPLACE'S EQUATION

By

YEN SEN WU

Lexington, Kentucky

Director: Dr. Frank J. Rizzo, Associate Professor

Lexington, Kentucky

A thesis submitted in partial fulfillment of the requirements for the degree of Master of Science in Engineering Mechanics at the University of Kentucky

1976

UNCLASSIFIED

SECURITY CLASSIFICATION OF THIS PAGE (When Data Entered)

REPORT DOCUMENTATION PAGE	READ INSTRUCTIONS BEFORE COMPLETING FORM
1. REPORT NUMBER (18) AFOSR - TR - 76 - 1313 (19)	2. GOVT ACCESSION NO. / 3. RECIPIENT'S CATALOG NUMBER
4. TITLE (and Subtitle) (6) THE BOUNDARY INTEGRAL EQUATION METHOD USING VARIOUS APPROXIMATION TECHNIQUES FOR PROBLEMS GOVERNED BY LAPLACE'S EQUATION.	5. TYPE OF REPORT & PERIOD COVERED (9) INTERIM rept., / 6. PERFORMING ORG. REPORT NUMBER
7. AUTHOR(s) (10) Yen Sen Wu	8. CONTRACT OR GRANT NUMBER(s) (15) AF-AFOSR 75-2824-75
9. PERFORMING ORGANIZATION NAME AND ADDRESS University of Kentucky Department of Engineering Mechanics Lexington, Kentucky 40506	10. PROGRAM ELEMENT, PROJECT, TASK AREA & WORK UNIT NUMBERS 681307 (16) 9782-04 (17) 04 61102F
11. CONTROLLING OFFICE NAME AND ADDRESS Air Force Office of Scientific Research/NA Building 410 Bolling Air Force Base, D.C. 20332	12. REPORT DATE (11) Dec 1976 / 13. NUMBER OF PAGES 102 (12) 104p.
14. MONITORING AGENCY NAME & ADDRESS(if different from Controlling Office)	15. SECURITY CLASS. (of this report) Unclassified / 15a. DECLASSIFICATION/DOWNGRADING SCHEDULE

16. DISTRIBUTION STATEMENT (of this Report)

Approved for public release; distribution unlimited

17. DISTRIBUTION STATEMENT (of the abstract entered in Block 20, if different from Report)

18. SUPPLEMENTARY NOTES

19. KEY WORDS (Continue on reverse side if necessary and identify by block number)

BOUNDARY VALUE PROBLEMS
PIECEWISE CONSTANT APPROXIMATION
QUADRATIC SHAPE FUNCTION
CUBIC SPLINE FUNCTION

20. ABSTRACT (Continue on reverse side if necessary and identify by block number)

The Boundary Integral Equation (BIE) method is applied to boundary value problems governed by Laplace's equation. In addition to the piecewise constant approximation for boundary functions, two other numerical approximations, quadratic shape function and cubic spline function representations, are adopted. Comparisons are discussed. Topics for further research are indicated.

DD FORM 1 JAN 73 1473 EDITION OF 1 NOV 65 IS OBSOLETE

UNCLASSIFIED 403077

SECURITY CLASSIFICATION OF THIS PAGE (When Data Entered)

ABSTRACT

THE BOUNDARY INTEGRAL EQUATION METHOD USING VARIOUS APPROXIMATION TECHNIQUES FOR PROBLEMS GOVERNED BY LAPLACE'S EQUATION

The Boundary Integral Equation (BIE) method is applied to boundary value problems governed by Laplace's equation. In addition to the piecewise constant approximation for boundary functions, two other numerical approximations, quadratic shape function and cubic spline function representations, are adopted. Comparisons are discussed. Topics for further research are indicated.

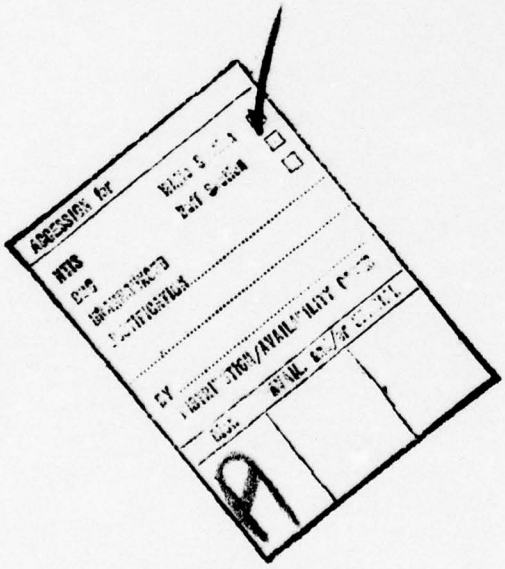

Author's Name

Date

TABLE OF CONTENTS

CHAPTER ONE

INTRODUCTION

Probably the most familiar partial differential equation of the elliptic type is Laplace's equation:

$$\nabla^2 U = 0$$

where $\nabla^2 \equiv \frac{\partial^2}{\partial x^2} + \frac{\partial^2}{\partial y^2} + \frac{\partial^2}{\partial z^2}$ for Cartesian coordinates.

It plays an important role in the various branches of the engineering and applied mathematics. It is satisfied, for example, if U is

(a) the temperature distribution under steady conditions in a region of constant conductivity;

(b) the warping function in the torsion of cylindrical bars;

(c) either the stream function or the velocity potential in the irrotational flow of an incompressible inviscid fluid;

(d) any distribution of electric potential in a region of constant resistivity;

(e) the distribution of magnetic potential in regions of constant permeability;

(f) either the real or imaginary part of any analytic function of a complex variable;

Therefore, the treatment of solutions to boundary value problems for this differential equation is interesting and important.

The methods of solution for such problems include analytical methods, graphical methods, numerical methods and analogical methods. For

the analytical approach, the method of separation of variables is used widely, where the general pattern yields different forms of solutions depending upon the nature of the problem and the particular coordinate systems involved. However, it is not always possible to separate variables [1][1]. As to another analytical approach, the similarity method, the similarity transformation [2] can be used via group theory such that Laplace's equation will be reduced to an ordinary differential equation easily. However, the capability of this transformation to properly carry over the boundary conditions to be compatible with the transformed equation is not always guaranteed. In fact, even though there are some other analytical approaches, e.g., the conformal mapping method [1], it turns out that the analytical approach is recommended only for dealing with problems which are simple in geometry and boundary conditions. When the geometry or boundary conditions become complicated, the analytical approach will be too involved to be practical.

For the graphical method [1], even with complex geometry, the problem will be easy to handle if the boundary conditions are uniform and normal derivatives of the potential function itself across the surface are zero. However, it will be awkward if the boundary conditions involved are not uniform or there are non-zero normal derivatives of the potential function across the surface. And even with simple

---

[1] Numbers in brackets indicate the references listed at the end of the text.

problems, the error of results can be very large without very great care in drawing.

The analogical method [3] can be applied to complicated problems, but sometimes the cost of construction of an analogue, obtaining the solutions in the analogous system, and translating them back into the original is tedious and not straightforward.

By considering all the advantages and disadvantages of the different approaches mentioned above, it is found by comparison that the numerical technique is generally the most desirable solution method, since it is flexible and is even applicable to systems with variable physical properties and nonuniform boundary conditions. More important, in recent years high-speed and large-capacity digital computers have developed rapidly and have become especially suitable for complicated and tedious numerical manipulations. Therefore the importance of the numerical method has grown greatly and will undoubtedly continue to grow at an increasing rate. Moreover, although the solution of problems using numerical methods does not provide general solutions as do the analytical methods, there are many situations for which numerical solutions provide the only approach which can be used. In fact, it is often found that when a general solution is known, it proves to be very difficult and tedious to translate into particular results for a particular problem; therefore, we may say that not only are numerical methods essential in problems which will not yield to any other method of solution, but that also they are often the best for obtaining a

particular solution even when a general solution is available by analytical methods. Moreover, it is usually the particular solution which the engineer and the physicist are interested in obtaining.

In the past, various numerical techniques have been applied to solve Laplacian problems. Among them, finite difference methods (FDM) and finite element methods (FEM) are popular, the practical difficulties associated with them being also well-known [4] [5]. However, by noticing that Laplace's equation is an elliptic type partial differential equation and therefore Laplacian problems are boundary value problems, a basic question will be raised: Is it possible to find a numerical technique which deals as much as possible only with the boundary data instead of referring at the outset to the whole domain, boundary and interior, as have been done in both FDM and FEM ? The answer is affirmative. Specifically, the boundary integral equation method (BIE) [6] is appropriate for this situation. The major feature of BIE is that unknown boundary data may be obtained by reference only to the boundary of the domain of interest without involving the interior. In essence, a given problem is solved on the boundary and the desired potential is evaluated at a desired interior point in terms of the boundary data. Obviously, the dimensions of the problem have been reduced by one. The great advantage to the analyst comes from simplification of the mathematical modelling. Thereafter, in this thesis, the BIE method will be applied to problems for Laplace's equation. Different approximation techniques used to carry out the

numerical analysis, having different features and advantages, will also be discussed.

In Chapter 2 we formulate boundary value problems for Laplace's equation, via the BIE, for two and three dimensional problems. Also we indicate a basic numerical procedure used with the BIE.

In Chapter 3 we discuss improved approximation methods, i. e. the quadratic shape function approximation for two and three dimensional problems and the spline function approximation for two dimensional problems. All procedures necessary to integrate the various kernel functions to form the elements of the matrix of coefficients in the resultant system of algebraic equations are presented in three Appendices. These procedures, though given in the Appendices to not interrupt the flow of the formulative ideas, are not merely detail. Indeed these procedures form the basis for actual numerical solutions as illustrated in section 3 of Chapter 3.

In Chapter 4 we offer some discussion and conclusions about the BIE vs. other numerical methods and about the various approximation methods used here. Some comments regarding extension of the presented methods for other classes of boundary value problems are also given.

CHAPTER TWO

BIE FORMULATION AND A BASIC NUMERICAL PROCEDURE

2.1 BIE FORMULATION

Consider the problem of determining a function $u(x_i)$ throughout a region R, i = 2 or 3 (for two-dimensional or three-dimensional regions, respectively), where u satisfies Laplace's equation

$$\nabla^2 u = 0 \qquad (x_i) \in R \qquad (2.1)$$

and R is a simply or multiply connected domain with boundary B. The boundary conditions are either of the Dirichlet type, of the form

$$u(x_i) = f(x_i) \qquad (x_i) \in B$$

or the Neumann type, of the form

$$\frac{\partial u(x_i)}{\partial n} = g(x_i) \qquad (x_i) \in B$$

or the Churchill type, of the form

$$u(x_i) = f(x_i) \qquad (x_i) \in B_1$$

$$\frac{\partial u(x_i)}{\partial n} = g(x_i) \qquad (x_i) \in B_2$$

where $B = B_1 + B_2$ and $\frac{\partial}{\partial n}$ is the derivative in the direction of the outward normal to the boundary. Functions $f(x_i)$ and/or $g(x_i)$ are prescribed on the boundary B, and for a well-posed boundary value problem $f(x_i)$ and $g(x_i)$ are not simultaneously prescribed over the same part of the boundary.

Now for any two sufficiently smooth and non-singular scalar functions U and V in R, it is well known from Green's theorem [7] that

$$\int_R (U \nabla^2 V - V \nabla^2 U) dR = \int_B (U \frac{\partial V}{\partial n} - V \frac{\partial U}{\partial n}) dB. \qquad (2.2)$$

For clarity, we now consider the two-dimensional and three-dimensional cases separately.

A. Two-Dimensional Case:

If we choose U = u(t), the harmonic function we are trying to determine, and V = log r(t, w) which is the fundamental singular solution to Laplace's equation in two dimensions (r(t, w) is the distance between any two points in the region), we will find that Eq. (2.2) will be invalid, because V will be singular when t coincides with w. Therefore we construct a small circle B′ with radius r′ around t as shown in Fig. 2.1,

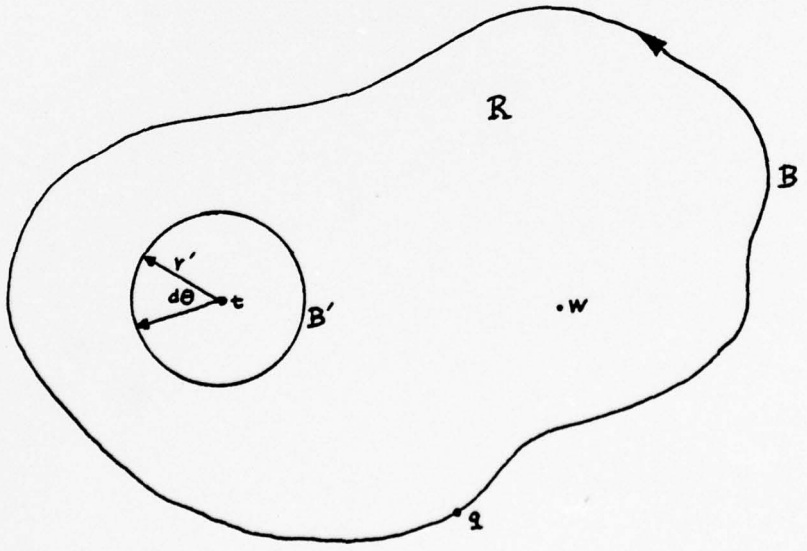

Fig. 2.1

and now Eq. (2.2) will be valid for the altered region. In addition, because both $\nabla^2 U$ and $\nabla^2 V$ are always zero, Eq. (2.2) can thus be written as

$$\int_{B+B'} [u(q) \frac{\partial \log r(t,q)}{\partial n} - \log r(t,q) \frac{\partial u(q)}{\partial n}] \, ds(q) = 0 \qquad (2.3)$$

where ds is the differential segment of boundary B. By taking the limit of the integrals over B′ as $r' \to 0$, it is found [7],

$$\lim_{r' \to 0} \int_{B'} u(q) \frac{\partial \log r'(t,q)}{\partial n} r'(t,q) d\theta(q) = -2\pi \, u(t) \qquad (2.4)$$

$$\lim_{r' \to 0} \int_{B'} \log r'(t,q) \frac{\partial u(q)}{\partial n} r'(t,q) d\theta(q) = 0 \qquad (2.5)$$

Combining Eqs. (2.3) (2.4) (2.5) gives an important relation which we will deal with later, i.e.,

$$u(t) = \frac{1}{2\pi} \int_B [u(q) \frac{\partial \log r(t,q)}{\partial n} - \log r(t,q) \frac{\partial u(q)}{\partial n}] \, ds \qquad (2.6)$$

This relation expresses an arbitrary harmonic function in terms of its boundary values and boundary values of its normal derivative.

However, as mentioned before, we know that for a well-posed boundary value problem, only "half" of the boundary data needed in Eq. (2.6) will be given; therefore it is obvious that Eq. (2.6) is not a solution to a given problem if we can not find a way to get the other half of the boundary data. In fact, how to find the other half of the boundary data is the basic idea of the BIE method.

Let p be a point lying on the boundary B, then by drawing a small circular bubble around p, there is a new boundary B′ + B″ as shown:

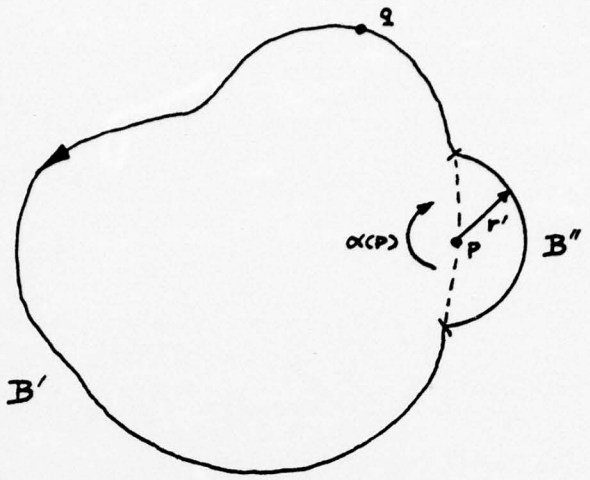

Fig. 2.2

According to the former derivation, we know that,

$$u(p) = \frac{1}{2\pi} \int_{B'+B''} [u(q) \frac{\partial \log r(p,q)}{\partial n} - \log r(p,q) \frac{\partial u(q)}{\partial n}] \, ds(q) \quad (2.7)$$

By taking the limit of the integrals over B' and B'' as $r' \to 0$ it is found [7] [8],

$$\lim_{r' \to 0} \int_{B''} u(q) \frac{\partial \log r'(p,q)}{\partial n} r'(p,q) d\theta(q) = (2\pi - \alpha(p)) u(p) \quad (2.8)$$

$$\lim_{r' \to 0} \int_{B''} \log r'(p,q) \frac{\partial u(q)}{\partial n} r'(p,q) d\theta(q) = 0 \quad (2.9)$$

where $\alpha(p)$ is the inner angle of p. Note that by considering a uniform distribution of u over the region mentioned, $\alpha(p)$ can be expressed as,

$$\alpha(p) = \int_B \frac{\partial \log r(p,q)}{\partial n} ds(q) \quad (2.10)$$

By combining Eqs. (2.7) (2.8) and (2.9), we arrive at the basic relationship of the BIE method,

$$u(p) = \frac{1}{\alpha(p)} \int_B [u(q) \frac{\partial \log r(p,q)}{\partial n} - \log r(p,q) \frac{\partial u(q)}{\partial n}] \, ds(q) \quad (2.11)$$

Eq. (2.11) gives us a linear relation between the boundary values of the harmonic function u(p) and those of its normal derivative $\frac{\partial u(p)}{\partial n}$. The essential concept of the BIE method is therefore the following: Specify the known boundary data in Eq. (2.11) and solve, by one of the numerical procedures to be discussed, for that part of the boundary data not initially prescribed. Once all boundary data is known, u(t) at any point t in R can be obtained by means of Eq. (2.6).

B. Three-Dimensional Case:

Let U = u(t), be the harmonic function to be determined, and V = 1/r (t, w) which is the fundamental singular solution to Laplace's equation in three dimensions (r(t, w) is the distance between any two points in the region). As in part A, Eq. (2.2) will be invalid for this region, so construct a small sphere B′ with radius r′ around t.

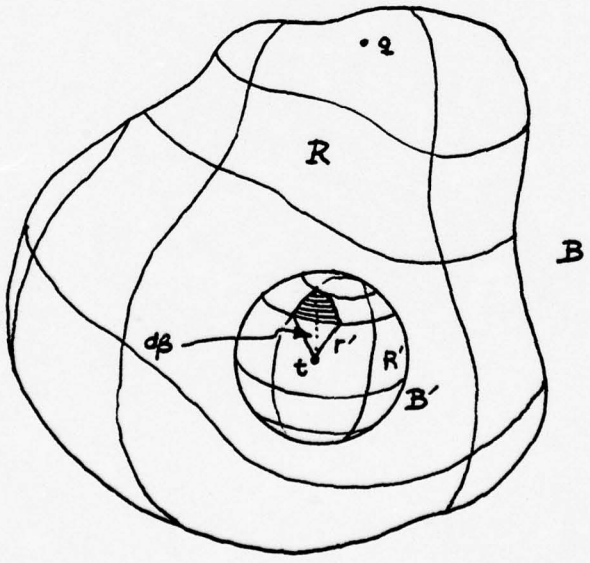

Fig. 2.3

Because $\nabla^2 U$ and $\nabla^2 V$ will be zero for the region R-R′, Eq. (2.2) can be written for the three-dimensional case as

$$\int_{B+B'} \left[u(q) \frac{\partial}{\partial n} \frac{1}{r(t,q)} - \frac{1}{r(t,q)} \frac{\partial u(q)}{\partial n} \right] da(q) = 0 \qquad (2.12)$$

where da is the differential area of boundary B. Taking the limit of the integral over B′ as before, it is found that [7]

$$\lim_{r' \to 0} \int_{B'} u(q) \frac{\partial}{\partial n} \frac{1}{r'(t,q)} - r'^2(t,q) d\beta = 4\pi u(t) \qquad (2.13)$$

$$\lim_{r' \to 0} \int_{B'} \frac{1}{r'(t,q)} \frac{\partial u(q)}{\partial n} r'^2(t,q) d\beta = 0 \qquad (2.14)$$

Combining Eqs. (2.12) (2.13) and (2.14), we thus have

$$u(t) = \frac{1}{4\pi} \int_B \left[\frac{1}{r(t,q)} \frac{\partial u(q)}{\partial n} - u(q) \frac{\partial}{\partial n} \frac{1}{r(t,q)} \right] da(q) \qquad (2.15)$$

Similarly, let p be a point on the boundary B. Construct a small bubble around p thus there will be a new boundary, B′+B″, with

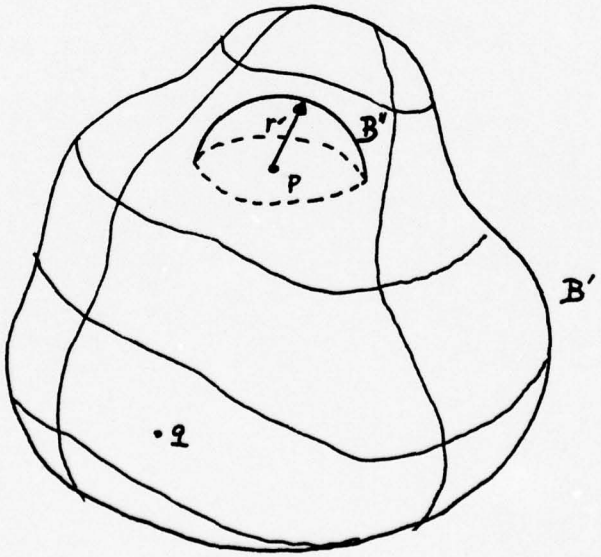

Fig. 2.4

$$u(p) = \frac{1}{4\pi} \int_{B'+B''} \left[\frac{1}{r(p,q)} \frac{\partial u(q)}{\partial n} - u(q) \frac{\partial}{\partial n} \frac{1}{r(p,q)} \right] da(q) \qquad (2.16)$$

and

$$\lim_{r' \to 0} \int_{B''} u(q) \frac{\partial}{\partial n} \frac{1}{r'(p,q)} r'^{2}(p,q) d\beta(q) = (\alpha(p) - 4\pi) u(p) \qquad (2.17)$$

$$\lim_{r' \to 0} \int_{B''} \frac{1}{r'(p,q)} \frac{\partial u(q)}{\partial n} r'^{2}(p,q) d\beta(q) = 0 \qquad (2.18)$$

where $\alpha(p)$, the inner solid angle of p, can be expressed as

$$u(p) = - \int_{B} \frac{\partial}{\partial n} \frac{1}{r(p,q)} da(q) \qquad (2.19)$$

Combining Eqs. (2.16) (2.17) and (2.18) we thus have

$$u(p) = \frac{1}{\alpha(p)} \int_{B} \left[\frac{1}{r(p,q)} \frac{\partial u(q)}{\partial n} - u(q) \frac{\partial}{\partial n} \frac{1}{r(p,q)} \right] da(q) \qquad (2.20)$$

Now, with the full formulation of interior-and boundary-boundary integral equations Eqs. (2.6), (2.11) and (2.15), (2.20), for the two-dimensional and three-dimensional Laplacian problems, respectively, we can go further to the numerical procedure.

2.2 A BASIC NUMERICAL PROCEDURE:

A Two-Dimensional Case:

The boundary B may be divided into N segments. Thus Eq. (2.11) can be written as

$$-u(p)\sum_{j=1}^{N}\int_{B_j}\frac{\partial \log r(p,q)}{\partial n}\,ds(q)+\sum_{j=1}^{N}\int_{B_j}u(q)\frac{\partial \log r(p,q)}{\partial n}\,ds(q)$$

$$=\sum_{j=1}^{N}\int_{B_j}\frac{\partial u(p)}{\partial n}\log r(p,q)\,ds(q) \qquad (2.21)$$

As a first approximation, each segment may be modelled as a straight line, and the function $u(q)$ and its normal derivative $u_n(q)$ over each segment may be considered constant, i.e., as the value at the mid-point of the segment.

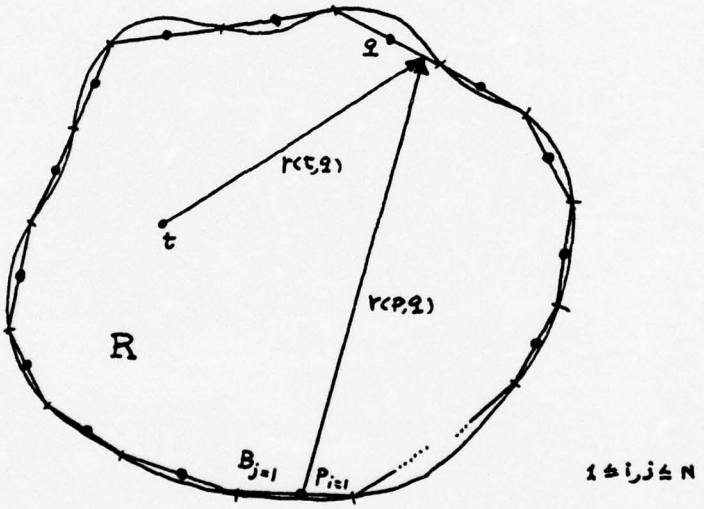

Fig. 2.5

Now, there will be N algebraic equations, each corresponding to the boundary-boundary integral equation (2.11) for point p at different segments:

$$-u(p_i)\sum_{j=1}^{N}\int_{B_j}\frac{\partial \log r(p_i,q)}{\partial n}\,ds(q)+\sum_{j=1}^{N}u_j\int_{B_j}\frac{\partial \log r(p_i,q)}{\partial n}\,ds(q)$$

$$=\sum_{j=1}^{N}u_{nj}\int_{B_j}\log r(p_i,q)\,ds(q)\qquad 1\le i\le N\qquad (2.22)$$

where u_j and u_{nj} are, respectively, are approximate values of u and its normal derivative over the jth segment. For conciseness, we can express the N linear simultaneous algebraic equations system of Eq. (2.22) in matrix form:

$$[A]\ \{U\}=[B]\ \{U_n\}\qquad (2.23)$$

where $[A]=[a_{ij}]\qquad 1\le i,j\le N$

$$\{U\}=\{u_j\}$$

$$[B]=[b_{ij}]$$

$$\{U_n\}=\{u_{n_j}\}$$

$$a_{ij}=\int_{B_j}\frac{\partial \log r(p_i,q)}{\partial n}\,ds(q)-\delta_{ij}\sum_{k=1}^{N}\int_{B_k}\frac{\partial \log r(p_i,q)}{\partial n}\,ds(q)\qquad (2.24)$$

$$b_{ij}=\int_{B_j}\log r(p_i,q)\,ds(q)\qquad (2.25)$$

Now, it is apparent that we can construct the [A] and [B] matrices numerically from Eqs. (2.24), (2.25) (Appendix 1). With the boundary data that is given, we can thus solve the Laplacian problem as follows.

For the Dirichlet problem, we have

$$\{C\} = [B]\ \{U_n\} \tag{2.26}$$

where $\{C\} = [A]\ \{U\}$

For the Neumann problem, we have

$$[A]\ \{U\} = \{C\} \quad \text{where } \{C\} = [B]\ \{U_n\} \tag{2.27}$$

However, note that the Neumann type problems do not have unique solutions, i.e., the [A] matrix is singular. Therefore, we should constrain arbitrarily one value of {U} so as to uniquely obtain all the other values of {U}. An easy way to do so is to specify one u to be zero, and eliminate the corresponding row and column in [A] and the corresponding element of {C}. We then deal with the reduced system, e.g.

$$[A^*]\ \{U^*\} = \{C^*\} \tag{2.28}$$

where $[A^*] = [a_{ij}]$ $\qquad 1 \le i, j \le N-1$

$$\{U^*\} = \{u_j\}$$

$$\{C^*\} = \{c_j\}$$

$$u_N = 0$$

Another way to do so is to specify arbitarily the value of one element of {U}, and assume the corresponding u_n to be unknown. We then solve the whole system as a mixed problem as described below.

For a mixed problem, we have

$$[A]\{U^*\} = \{C^*\} \tag{2.29}$$

where $[A^*] = [a^*_{ij}]$ $\qquad 1 \le i, j \le N$

$$\{U^*\} = \{u^*_j\}$$

$$\{C^*\} = [B^*]\{U^*_n\} = [b^*_{ij}]\{u^*_{nj}\}$$

For a segment where u is defined,

$$a^*_{ij} = b_{ij};\quad b^*_{ij} = a_{ij};\quad u^*_j = u_{nj};\quad u^*_{nj} = u_j$$

and for a segment where u_n is defined,

$$a^*_{ij} = a_{ij};\quad b^*_{ij} = b_{ij};\quad u^*_j = u_j;\quad u^*_{nj} = u_{nj}$$

Eq. (2.26) Eq. (2.28) or Eq. (2.29) can be solved by various standard methods. After application of the procedure mentioned above, the previously unknown boundary data is determined.

In terms of the discretized boundary and the entire boundary data, the interior field equation (2.6) can be thus written as

$$u(t) = \frac{1}{2\pi}\left[u_i k_{1i} - u_{n_i} k_{2i}\right] \qquad i \le i \le N \tag{2.30}$$

$$k_{1i} = \int_{B_i} \frac{\partial \log r(t,q)}{\partial n}\, ds(q) \tag{2.31}$$

$$k_{2i} = \int_{B_i} \log r(t,q)\, ds(q) \tag{2.32}$$

With Eqs. (2.30) (2.31) and (2.32) (Appendix 1), u(t), the solution of the Laplacian problem concerned, can be calculated anywhere of interest in the region R.

B. Three-Dimensional Case:

The boundary B may be divided into N segments. Thus Eq. (2.20) can be written as

$$-u(p)\sum_{j=1}^{N}\int_{B_j}\frac{\partial}{\partial n}\frac{1}{r(p,q)}\,da(q)+\sum_{j=1}^{N}\int_{B_j}u(q)\frac{\partial}{\partial n}\frac{1}{r(p,q)}\,da(q)$$

$$=\sum_{j=1}^{N}\int_{B_j}\frac{\partial u(q)}{\partial n}\frac{1}{r(p,q)}\,da(q) \qquad (2.33)$$

As a first approximation each segment may be modelled as a plane triangle, and the function u(q) and it's normal derivative $u_n(q)$ over each segment may be considered constant, i.e., as the value at the centroid of the segment.

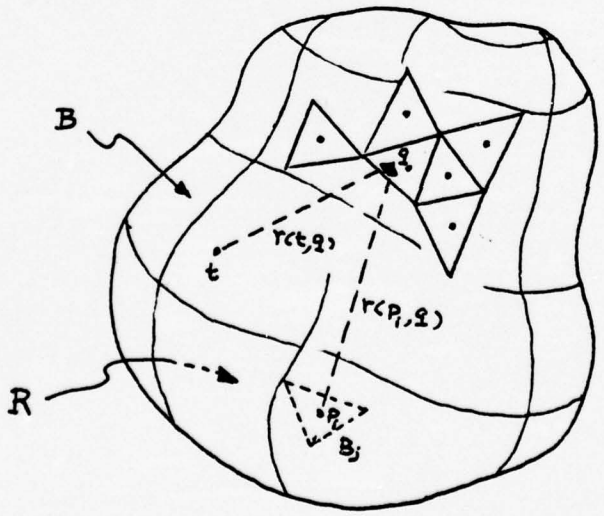

Fig. 2.6

Similar to the two-dimensional case, there will then be N algebraic equations, each corresponding to the boundary-boundary integral equation (2.19) for point p at different segments:

$$-u(p_i) \sum_{j=1}^{N} \int_{B_j} \frac{\partial}{\partial n} \frac{1}{r(p_i,q)}\, da(q) + \sum_{j=1}^{N} u_j \int_{B_j} \frac{\partial}{\partial n} \frac{1}{r(p_i,q)}\, da(q)$$

$$= \sum_{j=1}^{N} u_{nj} \int_{B_j} \frac{1}{r(p_i,q)}\, da(q) \qquad 1 \le i \le N \qquad (2.34)$$

In matrix form, Eq. (2.34) may be written as

$$[A]\{U\} = [B]\{U_n\} \qquad (2.35)$$

where $[A] = [a_{ij}]$ $\qquad 1 \le i, j \le N$

$$\{U\} = \{u_j\}$$

$$[B] = [b_{ij}]$$

$$\{U_n\} = \{u_{n_j}\}$$

and

$$a_{ij} = \int_{B_j} \frac{\partial}{\partial n} \frac{1}{r(p_i,q)}\, da(q) - \delta_{ij} \sum_{k=1}^{N} \int_{B_k} \frac{\partial}{\partial n} \frac{1}{r(p_i,q)}\, da(q) \qquad (2.36)$$

$$b_{ij} = \int_{B_j} \frac{1}{r(p_i,q)}\, da(q) \qquad (2.37)$$

Once the [A] and [B] matrices have been calculated numerically (Appendix 1) with half of the boundary data prescribed, the other half of the boundary data can be obtained numerically using the same procedures as in the two-dimensional case for Dirichlet, Neumann or mixed

type problems.

With the entire boundary data and the discretized boundary, the interior-boundary integral equation (2.15) can be expressed as

$$u(t) = \frac{1}{4\pi} \left[u_{n_i} k_{2i} - u_i k_{1i} \right] \qquad 1 \le i \le N \qquad (2.38)$$

$$k_{1i} = \int_{B_i} \frac{\partial}{\partial n} \frac{1}{r(t,q)} \, da(q) \qquad (2.39)$$

$$k_{2i} = \int_{B_i} \frac{1}{r(t,q)} \, da(q) \qquad (2.40)$$

As in the two-dimensional case, u(t) can be obtained anywhere of interest in the region R, with Eqs. (2.39) and (2.40) (Appendix 1).

CHAPTER III

IMPROVED APPROXIMATION METHODS

In the preceding chapter, for simplicity, we approximated the function u (q) and its normal derivative u_n (q) with constants over each segment. Obviously, in many cases this will be a very crude approximation particularly because of discontinuities. Therefore, improved approximation methods are desirable. There are various classes of approximating functions which could be used, for example, polynomials, trigonometric functions, exponentials, and rational functions. The most widely used approximating functions for well understood reasons are the polynomials which will also be our choice in this work.

As a first step, we will discuss what polynomials p(t) are good approximations to the real function f(t), i.e., u(q) and u_n (q) in our situation. Before that, we should make clear what is meant by a "good approximation" here.

Definition:

Let $f \in C^n(a,b)$ and define the norm $\| \quad \|_n$ of f as

$$\| f \|_n = \| f \| + \| f' \| + \| f'' \| + \cdots + \| f^{(n)} \|$$

where

$$\| f^{(j)} \| = \max_{t \in (a,b)} | f^{(j)}(t) |$$

A function g belonging to $C^n(a,b)$ is a good approximation to f, provided $\| f - g \|_n \leq \epsilon$ for a sufficiently small ϵ.

From the Weierstrass approximation theorem [9], which says for given any interval (a, b), any real number $\epsilon > 0$, and any real-valued function $f \in C^n(a, b)$, there exists a polynomial p(t) such that $\| f(t) - p(t) \| \angle \epsilon$ for all t in (a, b), we know that there do exist polynomials, p(t), which can be good approximations to the real function, f(t). The polynomial we are interested in is the interpolating polynomial.

Let $a = t_0 \angle t_1 \angle t_2 \angle \ \ldots \angle t_n = b$ be n + 1 distinct points on a closed interval (a, b) on a real axis and let f(t) be a real function defined at these points. It is obvious that there exist infinitely many polynomials p(t) which can approximate f(t) and interpolate f(t) at the points, $t_0, t_1, t_2, t_3, \ldots t_n$, where

$$p(t_i) = f(t_i) \qquad 0 \le i \le n$$

However, there is only one polynomial of degree $\le$ n which interpolates f(t) at these n + 1 distinct points. In terms of the Lagrange form, it will be

$$p(t) = f(t_k) l_k(t) \tag{3.1}$$

where

$$l_k(t) = \prod_{\substack{i=0 \\ i \neq k}}^{n} \frac{t - t_i}{t_k - t_i} \tag{3.2}$$

and

$$l_k(t_j) = \delta_{kj} \qquad 0 \le j \le n$$

$l_k(t)$ defined by (3.2) is called a Lagrange polynomial and is also known as a "shape function".

Although Lagrange polynomials are very easy to construct, an objection to this type of interpolating polynomial is that when the number of interpolating points becomes large, with a consequent high degree of Lagrange polynomial, calculation and evaluation of the interpolating polynomials become costly and, due to the propagation of errors, unreliable. Another more serious objection to the use of this interpolating polynomial of high degree is the fact that it may well increase the interpolating error. This can be easily seen by examining the error estimate for Lagrange polynomial p(t) which interpolates f(t) at $a = t_0 < t_1 < \ldots < t_n = b$. It is found [10] that, for $f \in C^{n+1}(a,b)$

$$\| f - p \| \leq \frac{\| f^{(n+1)} \|}{4(n+1)} h^{n+1}$$

for $f \in C^k(a,b) \quad 0 \leq k \leq n$

$$\| f - p \| \leq [1 + (\frac{2h}{h^*})^n] \, g_k(f,n)$$

where

$$h = \max_{0 \leq i \leq n-1} (t_{i+1} - t_i)$$

$$h^* = \min_{0 \leq i \leq n-1} (t_{i+1} - t_i)$$

$$g_k(f,n) = \begin{cases} 6w(f, \frac{b-a}{2n}) & k=0 \\ \frac{3(b-a)}{n} \| f' \| & k=1 \\ \frac{6^k (k-1)^{k-1}}{(k-1)! \, n^k} k(b-a)^k \| f^{(k)} \| & 1 < k \leq n \end{cases}$$

We can see then that the case of $f \in C^{n+1}(a,b)$, if $\| f^{(n+1)} \|$ increases sharply as n becomes large, reducing the size of h may prove to be of no help even if the knots are spaced optimally, e.g. [11]

$$\| f - p \| \leq \frac{\| f^{(n+1)} \|}{(n+1)} 2 \left(\frac{b - a}{4} \right)^{n+1}$$

where, the choice of Tchebycheff points for the interval (a,b) to minimize the approximating error are

$$t_j = \tfrac{1}{2}[b + a - (b - a)\cos[\frac{2j + 1}{2(n + 1)}\pi]] \qquad 0 \leq j \leq n$$

For $f \in C^k(a,b)$ $(0 \leq k \leq n)$ case, $[1 + (2h/h^*)^n]$ may grow too fast and outgrow the opposite effect due to $(b - a)/n$ for $k = 0$ and $((b - a)/n)^k$ for $1 \leq k \leq n$.

of course, error estimates are sometimes just pessimistic; however, from them we do find that there exists a way to guarantee the "smaller" error, even for small n. That way is to make the interval (a,b) small, and this leads to the "piecewise interpolating polynomial" idea. Based on this idea, we will go on to the following improved approximations.

3.1 SHAPE FUNCTION APPROXIMATION

A. Two-Dimensional Case:

As mentioned above, in order to have convergence as the number of segments increases, it would be necessary to use piecewise approximating polynomials. Within each subinterval, the shape function e.g., a Lagrange polynomial, can be constructed linearly, quadratically,

cubically, etc. The choice of degree depends on whether we want economic advantage or other advantages which can be achieved by increasing the number of degrees of freedom. Here we will choose the quadratic shape function to illustrate and apply the BIE method.

When we approximate the functions $u(q)$ and $u_n(q)$ by shape functions in terms of Lagrange polynomials, i.e.

$$u(q) = u(q_k) l_k(q)$$

$$u_n(q) = u_n(q_k) l_k(q)$$

over each segment, where $1 \le k \le 3$ for the quadratic Lagrange polynomial, and substitute into the two-dimensional boundary-boundary integral equation (2.11), it becomes

$$\alpha(p)u(p) = \sum_{i=1}^{N} \sum_{j=1}^{k} u(q_j) \int_{B_i} l_j(q) \frac{\partial \log r(p,q)}{\partial n} ds(q)$$

$$- \sum_{i=1}^{N} \sum_{j=1}^{k} u_n(q_j) \int_{B_i} l_j(q) \log r(p,q) ds(q)$$

However, it is found that unless the boundary segment is a straight line or we are going to model the curved boundary segments as straight lines as we did in Chapter 2, it will be difficult to perform the approximate integration over each segment if we do not know the geometric expression for the boundary, which is frequently the case. In turn, this will be a drawback if we want to use a computer-aided program to make the geometric partition of the boundary so as to gain efficiency. Therefore, a parametric transformation should be used initially to

transform the given arbitrary boundary segment into a standard boundary segment to which a rule of approximation integration, like the Gaussian quadrature we shall adopt, can be readily applied. In fact, this can be done by using the so-called "isoparametric transformation" [12], where we use the shape functions used to approximate the functions to also approximate the boundary geometry.

For this purpose, let the standard boundary segment be described by the curvilinear coordinate e as shown in Fig. 3.1. The quadratic shape functions related to this coordinate are

$$N^1(e) = -\tfrac{1}{2}e + \tfrac{1}{2}e^2$$

$$N^2(e) = 1 - e^2 \qquad (3.3)$$

$$N^3(e) = \tfrac{1}{2}e + \tfrac{1}{2}e^2$$

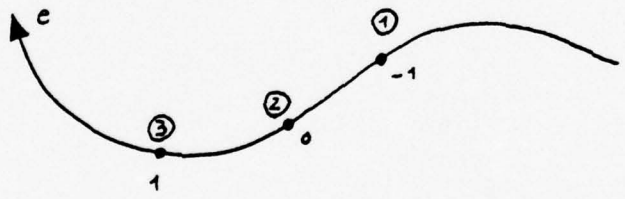

Fig. 3.1

The x and y coordinates and functions u(q), $u_n(q)$ can thus be approximated as

$$x(e) = N^{\alpha}(e)x^{\alpha}$$

$$y(e) = N^{\alpha}(e)y^{\alpha} \tag{3.4}$$

$$u(e) = N^{\alpha}(e)u^{\alpha}$$

$$u_n(e) = N^{\alpha}(e)\, u_n^{\alpha} \tag{3.5}$$

where x^{α}, y^{α}, u^{α}, u_n^{α} are the function values defined at the nodes of the boundary, and $1 \le \alpha \le 3$ for the quadratic case. It is also found that

$$ds(q(e)) = J(e)de \tag{3.6}$$

where

$$J(e) = \sqrt{\left(\frac{dx}{de}\right)^2 + \left(\frac{dy}{de}\right)^2}$$

$$= \sqrt{\left(\frac{dN^{\alpha}(e)}{de}\, x^{\alpha}\right)^2 + \left(\frac{dN^{\alpha}(e)}{de}\, y^{\alpha}\right)^2} \tag{3.7}$$

Before we apply these shape function expressions to the boundary- and interior-boundary integral equations, we will further look at the boundary-boundary integral equations. It is found that, by using Eq. (2.11) Eq. (2.10) can be written as

$$\int_B [u(q) - u(p)] \frac{\partial \log r(p,q)}{\partial n} ds(q) = \int_B u_n(q) \log r(p,q) ds(q) \tag{3.8}$$

Now by substituting Eqs. (3.5) (3.6) into Eq. (3.8) for each specific point p, Eq. (3.8) can be formulated as

$$\sum_{j=1}^{N}\sum_{\alpha=1}^{3} u^{j(\alpha)} \int_{B_j'} N^{\alpha}(e) \frac{\partial \log r(p_i, q(e))}{\partial n} J(e)de \qquad 1\le i, j(\alpha) \le 2N$$

$$- u(p_i) \sum_{j=1}^{N} \int_{B_j'} \frac{\partial \log r(p_i, q(e))}{\partial n} J(e)de$$

$$= \sum_{j=1}^{N}\sum_{\alpha=1}^{3} u_n^{j(\alpha)} \int_{B_j'} N^{\alpha}(e) \log r(p_i, q(e)) J(e)de \qquad (3.9)$$

where N is the number of segments and B_j' is the j^{th} standard boundary segment with limits (-1, 1). In short, Eq. (3.9) can be expressed as

$$\sum_{j=1}^{N} \left[\sum_{\alpha=1}^{3} u^{j(\alpha)} a_{ij}^{\alpha} - u(p_i) a_{ij}' \right]$$

$$= \sum_{j=1}^{N}\sum_{\alpha=1}^{3} u_n^{j(\alpha)} b_{ij}^{\alpha} \qquad (3.10)$$

Since a_{ij}^{α}, a_{ij}', b_{ij}^{α} can be calculated numerically (Appendix 2), we can thus form Eq. (3.10) in matrix form as

$$[A]\{U\} = [B]\{U_n\} \qquad (3.11)$$

Thus, for either Dirichlet or Neumann or mixed type problems the unknown half of the boundary data can be obtained by the procedure described in Sec. 2.2.

With all these boundary data, u^m and u_n^m, $1 \le m \le 2N$, the two-dimensional Laplacian problem can thus be solved by the use of the Interior-boundary integral equation (2.6), which can be expressed as

$$u(t) = \frac{1}{2\pi} \sum_{j=1}^{N} \sum_{\alpha=1}^{3} [\, u^{j(\alpha)} k_{1j}^{\alpha} - u_n^{j(\alpha)} k_{2j}^{\alpha} \,] \tag{3.12}$$

where

$$k_{1j}^{\alpha} = \int_{B'j} N^{\alpha}(e) \frac{\partial \log r(t, q(e))}{\partial n} \, de \tag{3.13}$$

$$k_{2j}^{\alpha} = \int_{B'_j} N^{\alpha}(e) \log r(t, q(e)) J(e) de \tag{3.14}$$

can be calculated numerically (Appendix 2).

B. Three-Dimensional Case:

Unlike the two-dimensional case, here we deal with the integration over curved surface boundaries where a boundary segment could be a curvilinear triangle, quadrilateral ... etc. Here the boundary segment we will use will be a quadrilateral. Similar to the two-dimensional case, in order to perform the numerical integration and the automatic mesh generation, the parametric transformation is used. Also, we let $B'_j = (-1,1)x(-1,1)$, the curvilinear quadrilateral with curvilinear coordinates e, f, be the standard boundary segment as shown in Fig. 3.2.

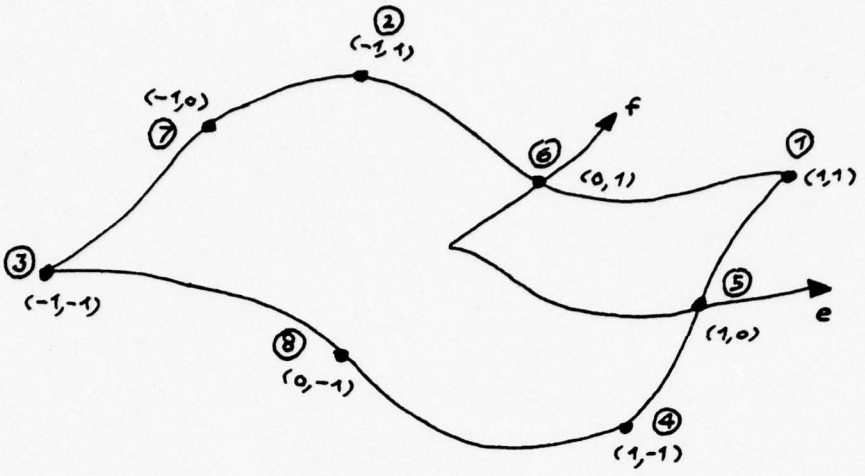

Fig. 3.2

Based upon this standard boundary segment, we could easily construct the two-dimensional shape functions by forming the tensor product of the appropriate one-dimensional Lagrangian shape functions which we used before. However, due to the larger number of degrees of freedom involved we will not proceed this way. Instead, we will choose the Serendipity's elements [13] for our usage, where, for the biquadratic approximation, the shape functions can be expressed as

$$N^{\alpha}(e,f) = \tfrac{1}{4}(1 + e_0)(1 + f_0)(e_0 + f_0 - 1) \qquad 1 \le \alpha \le 4$$

$$N^{\alpha}(e,f) = \tfrac{1}{2}(1 + e_0)(1 - f^2) \qquad \alpha = 5, 7$$

$$N^{\alpha}(e,f) = \tfrac{1}{2}(1 - e^2)(1 + f_0^2) \qquad \alpha = 6, 8 \qquad (3.15)$$

where

$$e_0 = ee^{\alpha}$$

$$f_0 = ff^{\alpha}$$

For the isoparametric transformation, the x and y and z geometric coordinates and functions u(q), $u_n(q)$ can be approximated as

$$x(e,f) = N^{\alpha}(e,f)x^{\alpha}$$

$$y(e,f) = N^{\alpha}(e,f)y^{\alpha}$$

$$z(e,f) = N^{\alpha}(e,f)z^{\alpha} \tag{3.16}$$

$$u(e,f) = N^{\alpha}(e,f)u^{\alpha}$$

$$u_n(e,f) = N^{\alpha}(e,f)u_n^{\alpha} \tag{3.17}$$

where x^{α}, y^{α}, z^{α}, u^{α}, u_n^{α}, as before, are the function values defined at the nodes of the boundary nodes shown as Fig. 3.2. Also, it is found that (Appendix 2).

$$da(q(e,f)) = J(e,f)de\ df \tag{3.18}$$

where

$$J(e,f) = \sqrt{N_1^{*2} + N_2^{*2} + N_3^{*2}} \tag{3.19}$$

$$N_1^* = (\alpha_2\beta_3 - \alpha_3\beta_2)$$

$$N_2^* = (\alpha_3\beta_1 - \alpha_1\beta_3)$$

$$N_3^* = (\alpha_1\beta_2 - \alpha_2\beta_1)$$

$$\begin{bmatrix} \alpha_1 & \alpha_2 & \alpha_3 \\ \beta_1 & \beta_2 & \beta_3 \end{bmatrix} = \begin{bmatrix} \frac{\partial N^{\alpha}(e,f)}{\partial e} \\ \frac{\partial N^{\alpha}(e,f)}{\partial f} \end{bmatrix} [x^{\alpha}, y^{\alpha}, z^{\alpha}]$$

Similar to the two-dimensional case, it is found that by using Eq. (2.19), Eq. (2.20) can be rewritten as

$$\int_B [u(q) - u(p)] \frac{\partial}{\partial n} \frac{1}{r(p,q)} da(q) = \int_B u_n(q) \frac{1}{r(p,q)} da(q) \tag{3.20}$$

By substituting Eqs. (3.17), (3.18) into Eq. (3.20) for each specific point p, Eq. (3.20) can be expressed as

$$\sum_{j=1}^{N} \sum_{\alpha=1}^{8} u^{j(\alpha)} \int_{B'_j} N^{\alpha}(e,f) \frac{\partial}{\partial n} \frac{1}{r(p_i, q(e,f))} J(e,f) de\, df$$

$$- u(p_i) \sum_{j=1}^{N} \int_{B'_j} \frac{\partial}{\partial n} \frac{1}{r(p_i, q(e,f))} J(e,f) de\, df \qquad 1 \le i, j(\alpha) \le NN$$

$$= \sum_{j=1}^{N} \sum_{\alpha=1}^{8} u_n^{j(\alpha)} \int_{B'_j} N^{\alpha}(e,f) \frac{1}{r(p_i, q(e,f))} J(e,f) de\, df \tag{3.21}$$

where N is the number of segments, NN is the total number of nodes, and B'_j is the j^{th} standard boundary segment with limits (-1, 1)x(-1, 1). Eq. (3.21) can be expressed in the abbreviated form

$$\sum_{j=1}^{N} \left[\sum_{\alpha=1}^{8} u^{j(\alpha)} a_{ij}^{\alpha} - u(p_i) a'_{ij} \right] = \sum_{j=1}^{N} \sum_{\alpha=1}^{8} u_n^{j(\alpha)} b_{ij}^{\alpha} \tag{3.22}$$

After a'_{ij}, a_{ij}^{α}, b_{ij}^{α} have been calculated numerically (Appendix 2). Eq. (3.22) can be written in matrix form as

$$[A] \{U\} = [B] \{U_n\} \tag{3.23}$$

which can be solved as described previously.

When all the boundary data have been obtained, the three-dimensional Laplacian problem can then be solved by use of the interior-boundary integral equation (2.15)

$$u(t) = \frac{1}{4\pi} \sum_{j=1}^{N} \sum_{\alpha=1}^{8} [\, u_n^{j(\alpha)} k_{2j}^{\alpha} - u^{j(\alpha)} k_{ij}^{\alpha} \,] \tag{3.24}$$

where

$$k_{1j}^{\alpha} = \int_{B'_j} N^{\alpha}(e,f) \frac{\partial}{\partial n} \frac{1}{r(t,q(e,f))} J(e,f)\,de\,df \tag{3.25}$$

$$k_{2j}^{\alpha} = \int_{B'_j} N^{\alpha}(e,f) \frac{1}{r(t,q(e,f))} J(e,f)\,de\,df \tag{3.26}$$

can be calculated numerically (Appendix 2).

3.2 SPLINE FUNCTION APPROXIMATION

By examining the shape function approximations used in last section, it is found that both the Lagrange or the Serendipity type, guarantee continuity of only the function itself at the "knots", where a "knot" is a point at which the piecewise-smooth polynomials are joined together. Consider the one-dimensional, piecewise-quadratic shape function of Lagrange's family, for example, as shown in Fig. 3.3, where $l_j^i(t)$ is the quadratic Lagrange's polynomial over the i^{th} interval.

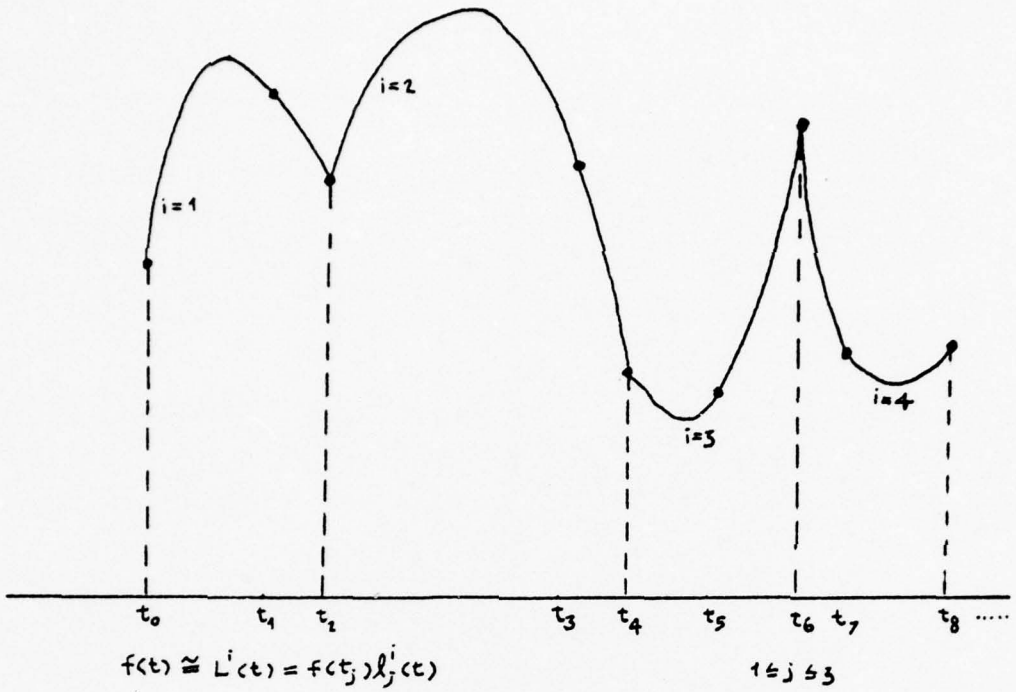

Fig. 3.3

It has been noticed that there exist sharp corners at these knots (t_2, t_4, t_6, ...) due to the lack of differentiability of $L^i(t)$ at the knots. Of course, if the approximated function is smooth, then the drawback of lack of smoothness will cause trouble when the solutions found numerically have to be differentiated at the knots. Therefore, it may be desirable to use approximating functions which are not only continuous at the knots but also have continuous derivatives at the knots.

There are various ways to achieve the smoothness requirements for the piecewise polynomials. One way is to use values of derivatives as well as the function itself. However, if spline functions are used, these requirements can be met by using only values of the function itself [14], [15], [16], [17]. As Schoenberg pointed out, the fundamental

properties of spline functions, as a class of piecewise polynomial functions with continuity properties of the function itself and its derivatives, are simple and the mathematics involved elementary. In recent years, there have been numerous works with regard to the development of the theory of approximation by splines.

Here, we will look at the cubic B-spline first. It is known as the basic spline, because Schoenberg has proved that every cubic spline can be written as a linear combination of B-splines. By considering a partition over the interval $a = t_1 \leq t_2 \leq t_3 \leq \ldots \leq t_n = b$ with evenly spaced subintervals, the B-spline, $B_i(t)$, is defined as

$$B_i(t) = \begin{cases} (t - t_{i-2})^3 & t \in (t_{i-2}, t_{i-1}) \\ h^3 + 3h^2(t - t_{i-1}) + 3h(t - t_{i-1})^2 - 3(t - t_{i-1})^3 & t \in (t_{i-1}, t_i) \\ h^3 + 3h^2(t_{i+1} - t) + 3h(t_{i+1} - t)^2 - 3(t_{i+1} - t)^3 & t \in (t_i, t_{i+1}) \\ (t_{i+2} - t)^3 & t \in (t_{i+1}, t_{i+2}) \\ 0 & \text{otherwise} \end{cases} \qquad (3.27)$$

This function is represented graphically in Fig. 3.4.

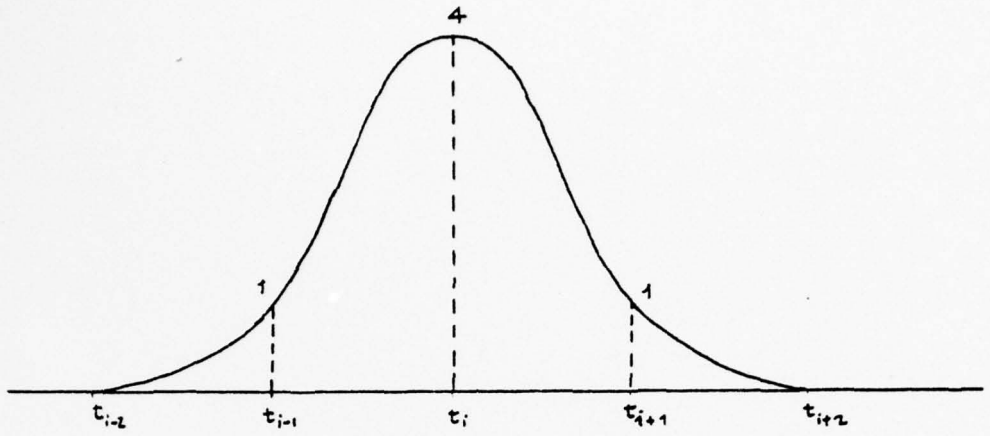

Fig. 3.4

As mentioned before, any cubic spline s(t) can be expressed as a linear combination of cubic B splines (cf. Fig. 3.5):

$$s(t) = \sum_{i=0}^{n+1} a_i B_i(t) \tag{3.28}$$

where a_0 and a_{n+1}, the two additional flexible degrees of freedom, are caused by the not strictly local property of B splines.

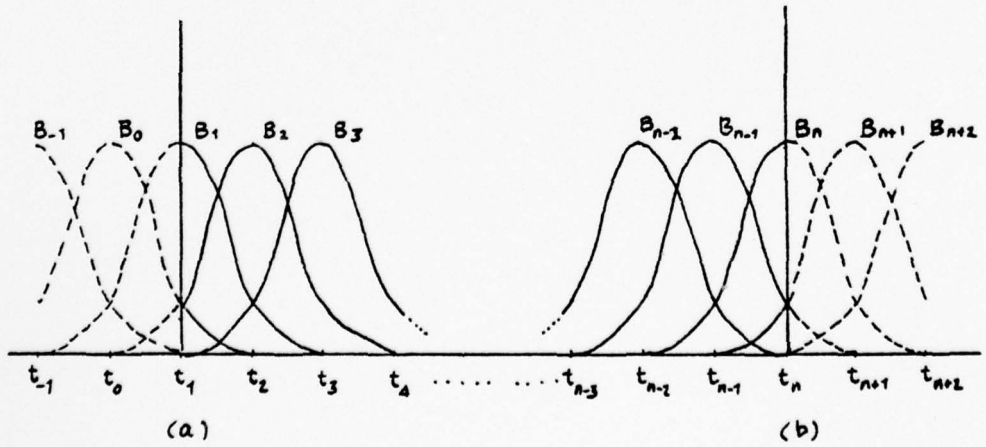

Fig. 3.5

To determine all the coefficients a_i, besides the original data, e.g. $s(t_i)$, $1 \le i \le n$, a choice of the two extra degrees of freedom should be made, e.g., $s'(t_1) = f'(t_1)$, $s'(t_n) = f'(t_n)$ or $s''(t_1) = f''(t_1)$ $s''(t_n) = f''(t_n)$ etc., as the extreme boundary condition, the periodic case as shown in Fig. 3.6.

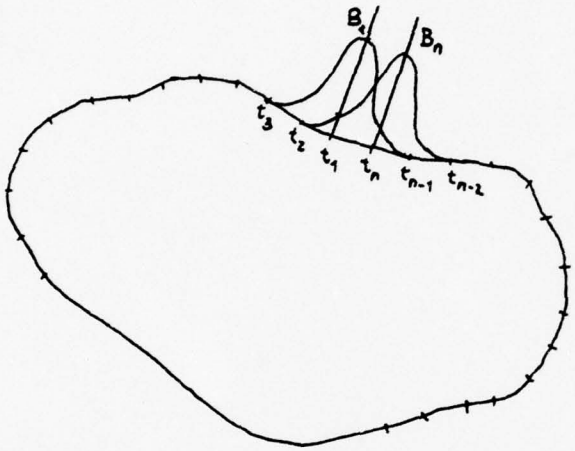

Fig. 3.6

It is found that Eq. (3.28) can be reduced to

$$s(t) = \sum_{i=1}^{n} a_i B_i(t)$$

due to the periodic properties, i.e., $t_0 = t_n$, $t_{n+1} = t_1$ and $B_0(t) = B_n(t)$.

$$B_{n+1}(t) = B_1(t).$$

For our purpose, we will use the periodic spline with equal intervals. Therefore, in terms of cubic B splines the potential function u(q) and its normal derivative $u_n(q)$ for a specific closed boundary can be approximated as

$$u(s) = \sum_{j=1}^{N} e_j B(s - s_j)$$

$$u_n(s) = \sum_{j=1}^{N} f_j B(s - s_j) \tag{3.29}$$

where s is the curvilinear coordinate of the specific closed boundary:

$$B(s - s_j) = \left\{ \begin{array}{l} 0 \\ B_1(s - s_j) \\ \\ \\ B_2(s - s_j) \\ \\ \\ B(s_j - s) \end{array} \right\} = \left\{ \begin{array}{ll} 0 & 2h \le (s - s_j) \\ (2 - \frac{(s - s_j)}{h})^3 & \\ & h \le (s - s_j) \le 2h \\ (2 - \frac{(s - s_i)^3}{h} - 4(1 - \frac{(s - s_j)}{h})^3 & \\ & 0 \le (s - s_j) \le h \\ B(s_j - s) & s - s_j \le 0 \end{array} \right. \tag{3.30}$$

and h is the length of the equal intervals between nodes.

Substituting Eq. (3.29) into the two-dimensional boundary-boundary integral equation (2.11) results in

$$\alpha(p_i) \sum_{j=1}^{N} e_j B(p_i - s_j) - \int_B \sum_{j=1}^{N} e_j B(q(s) - s_j) \frac{\partial \log r(p_i, q(s))}{\partial n} ds$$

$$= - \int_B \sum_{j=1}^{N} f_j B(q(s) - s_j) \log r(p_i, q(s)) ds. \tag{3.31}$$

After careful rearrangement, it is found that Eq. (3.31) can be expressed in the matrix form

$$[A]\{E\} = [B]\{F\} \tag{3.32}$$

where

$$[A] = [a_{ij}]; \quad \{E\} = \{e_j\}\ ; \ [B] = [b_{ij}]; \quad \{F\} = \{f_j\}$$

$$a_{ij} = \begin{cases} 4\pi + \bar{a}_{ij} & \text{when } B_i = B_j \\ \pi + \bar{a}_{ij} & \text{when } B_i \text{ and } B_j \text{ are neighbor interval} \\ \bar{a}_{ij} & \text{otherwise} \end{cases}$$

$$\begin{aligned} \bar{a}_{ij} = &- \int_{B_j} B_2 (s - s_j) \frac{\partial \log r(p_i, q(s))}{\partial n} ds \\ &- \int_{B_{j+1}} B_1(s - s_j) \frac{\partial \log r(p_i, q(s))}{\partial n} ds \\ &- \int_{B_{j-1}} B_2(s_j - s) \frac{\partial \log r(p_i, q(s))}{\partial n} ds \\ &- \int_{B_{j-2}} B_1(s_j - s) \frac{\partial \log r(p_i, q(s))}{\partial n} ds \end{aligned} \tag{3.33}$$

$$b_{ij} = -\int_{B_j} B_2(s - s_j)\log r(p_i, q(s))ds$$

$$- \int_{B_{j+1}} B_1(s - s_j)\log r(p_i, q(s))ds$$

$$- \int_{B_{j-1}} B_2(s_j - s)\log r(p_i, q(s))ds$$

$$- \int_{B_{j-2}} B_1(s_j - s)\log r(p_i, q(s))ds \qquad (3.34)$$

$\bar{a}_{ij}$, b_{ij} can be calculated numerically (Appendix 3).

From Eqs. (3.24), (3.30), we know that

$$\{U\} = [D]\ \{E\}$$

$$\{U_n\} = [D]\ \{F\}$$

where

$$[D] = \begin{bmatrix} 4\ 1\ 0\ 0 \ldots\ldots\ldots\ldots\ldots 1 \\ 1\ 4\ 0\ 0 \ldots\ldots\ldots\ldots\ldots 0 \\ 0\ 1\ 4\ 1 \ldots\ldots\ldots\ldots\ldots 0 \\ 0\ 0\ 1\ 4 \ldots\ldots\ldots\ldots\ldots 0 \\ \cdot\ \cdot\ \cdot\ \cdot \ldots\ldots\ldots\ldots\ldots \cdot \\ \cdot\ \cdot\ \cdot\ \cdot \ldots\ldots\ldots\ldots\ldots \cdot \\ \cdot\ \cdot\ \cdot\ \cdot \ldots\ldots\ldots\ldots\ldots \cdot \\ 1\ 0\ 0\ 0 \ldots\ldots\ldots\ldots\ldots 14 \end{bmatrix}$$

Therefore, Eq. (3.32) can be rewritten as

$$[A][D]^{-1}\ \{U\} = [B]\ [D]^{-1}\ \{U_n\}$$

i.e.

$$[\bar{A}]\ \{U\} = [\bar{B}]\ \{U_n\} \tag{3.35}$$

Then, by the similar procedures mentioned in Sec. 2.2, all the necessary boundary data can be obtained. It should be pointed out that a multiply connected region can also be handled by generalizing the procedure mentioned above.

After all the u_j and u_{n_j} have been determined, the two-dimensional Laplacian problem can be solved by substituting Eq. (3.29) into the two-dimensional interior-boundary integral equation (2.6) as

$$u(t) = \frac{1}{2\pi}\left[\int_B \sum_{j=1}^{N} e_j B(q(s) - s_j)\ \frac{\partial \log r(t, q(s))}{\partial n}\, ds\right.$$

$$\left. - \int_B \sum_{j=1}^{N} f_j B(q(s) - s_j) \log r(t, q(s)) ds\right] \tag{3.36}$$

i.e.

$$u(t) = \frac{1}{2\pi}\ [k_{1j} e_j - k_{2j} f_j] \tag{3.37}$$

where

$$k_{1j} = \int_{B_j} B_2(s - s_j) \frac{\partial \log r(t,q(s))}{\partial n} ds$$

$$+ \int_{B_{j+1}} B_1(s - s_j) \frac{\partial \log r(t,q(s))}{\partial n} ds$$

$$+ \int_{B_{j-1}} B_2(s_j - s) \frac{\partial \log r(t,q(s))}{\partial n} ds$$

$$+ \int_{B_{j-2}} B_1(s_j - s) \frac{\partial \log r(t,q(s))}{\partial n} ds \qquad (3.38)$$

$$k_{2j} = \int_{B_j} B_2(s - s_j) \log r(t,q(s)) ds$$

$$+ \int_{B_{j+1}} B_1(s - s_j) \log r(t,q(s)) ds$$

$$+ \int_{B_{j-1}} B_2(s_j - s) \log r(t,q(s)) ds$$

$$+ \int_{B_{j-1}} B_1(s_j - s) \log r(t,q(s)) ds \qquad (3.39)$$

can be calculated numerically (Appendix 3), and $\{e_j\}$ and $\{f_j\}$ can be obtained via

$$\{e_j\} = [D]^{-1} \{u_j\}$$

$$\{f_j\} = [D]^{-1} \{u_{n_j}\}$$

3.3 TEST PROBLEMS:

3.3.1 Two-Dimensional Case:

(a) Consider the temperature distribution along the boundary of a circular disk (see Fig. 3.7) to be maintained as $u(r_o, \theta) = \sin\theta$.

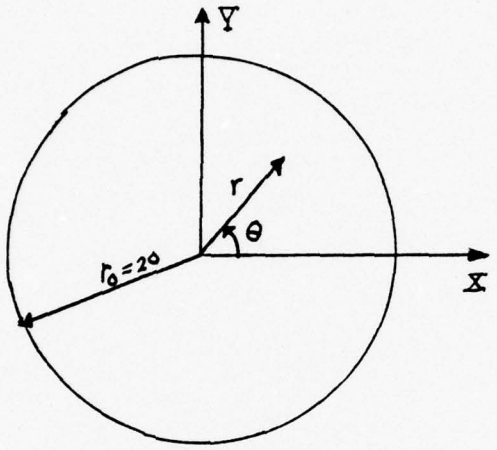

Fig. 3.7

The exact analytical solution is $u(r, \theta) = (r/r_o) \sin\theta$ and it is desired to solve for the boundary heat flux by using the BIE method with piecewise-constant approximation, quadratic shape function approximation and cubic spline function approximation. Comparisons are listed in the table below.

Approximation method	Boundary points used	Average relative error	Computing time
Constant	10	8.61%	0.25 sec.
	20	2.04%	0.64 sec.
	40	0.49%	0.84 sec.
	80	0.11%	3.25 sec.
Quadratic shape function	10	0.35%	0.21 sec.
	20	0.10%	1.18 sec.
	40	0.04%	4.13 sec.
Cubic spline function	10	1.13%	0.94 sec.
	20	0.11%	3.68 sec.
	40	0.01%	3.95 sec.

All the relative errors listed in Sec. 3.3 are taken as the absolute value of the ratio of the difference between the analytical solution and numerical solution to the analytical solution. Regarding the boundary solutions, all the relative errors at each boundary point are then averaged.

Unless otherwise mentioned, the Gaussian points (Appendix 2) used in Sec. 3.3 are 4 and 4 x 4 for the quadratic shape function approximation and biquadratic shape function approximation, respectively.

(b) Consider a circular ring, a multi-connected region, with different constant temperatures along the inner and outer boundaries, as shown in Fig. 3.8.

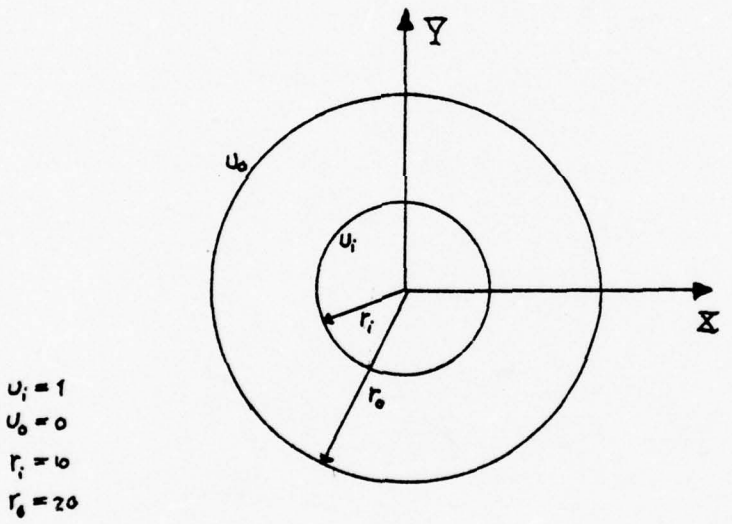

Fig. 3.8

The exact analytical solution is $u(r) = u_i + (u_o - u_i) \ln (r/r_i)/\ln (r_o/r_i)$. We solve for the boundary heat flux by using the BIE method with piecewise constant approximation, quadratic shape function approximation and cubic spline function approximation. The comparisons are listed in the table below:

Approximation method	Boundary points used	Average relative error	Computing time
Constant	20	2.3%	0.6 sec.
Quadratic shape function	20	0.1%	1.2 sec.
Cubic spline function	20	1.6%	1.4 sec.

(c) Consider a rectangle, kept at different constant temperatures on two opposite surfaces and insulated on the other two opposite sides

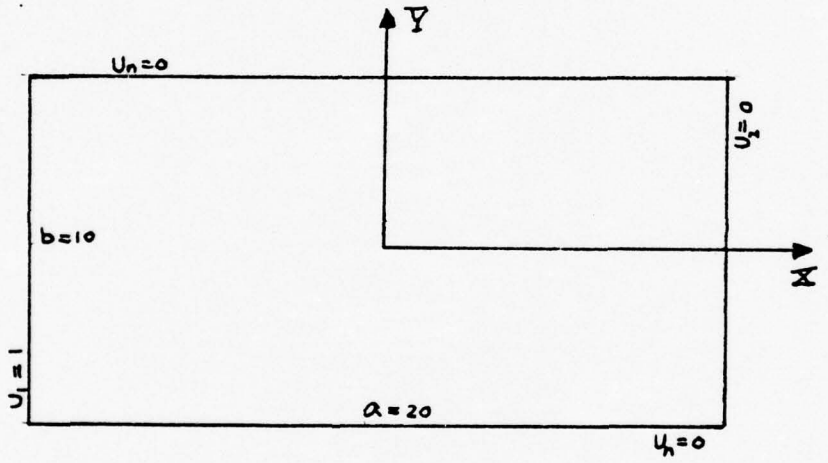

Fig. 3.9

The exact analytical solution is $u = (u_2 + u_1)/2 + (u_2 - u_1)x/a$.

It is desired to solve, by using piecewise constant approximation and quadratic shape function approximation, partly for the boundary temperatures and partly for the heat flux and then solve for some interior temperatures. Results are shown in the tables below:

Piecewise Constant Approximation
(16 boundary points used)
(0.43 sec. computing time)

Interior Coordinates		Analytical Solution	Numerical Solution	Relative Error
x	y			
6.0	0	0.2000	0.1965	1.8%
0	0	0.5000	0.5000	0
-4.0	3.0	0.7000	0.7005	0.1%

Quadratic Shape Function Approximation
(16 boundary points used)
(1.06 sec. computing time)

Interior Coordinates		Analytical Solution	Numerical Solution	Relative Error
x	y			
6.0	0	0.2000	0.1983	0.8%
0	0	0.5000	0.4989	0.2%
-4.0	3.0	0.7000	0.7011	0.1%

3.3.2 Three-Dimensional Case:

(a) Consider a cube, kept at different constant temperatures on 2 opposite surfaces with temperature varied lineary along the other four adjacent surfaces, according to $u - u_2 + (u_1 - u_2)x/a$ as shown in Fig. 3.10.

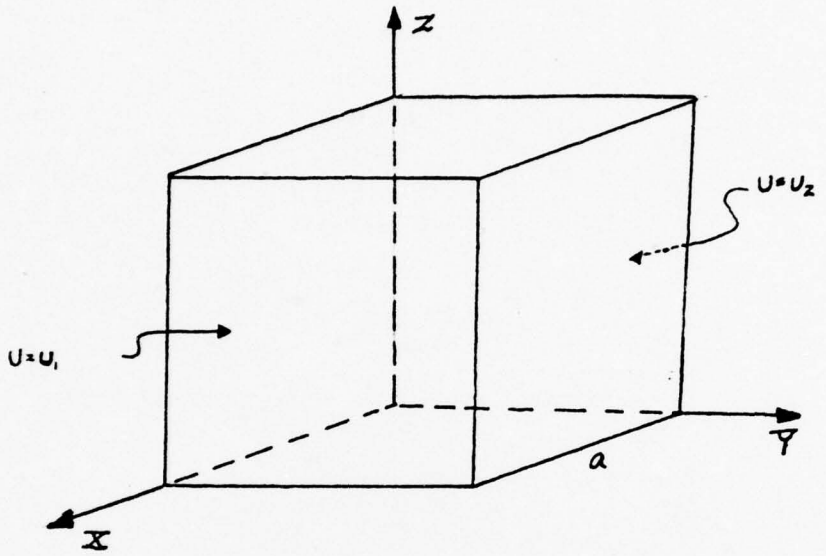

Fig. 3.10

We solve for the boundary heat flux by using the BIE method with piecewise constant approximation and biquadratic shape function approximation. The comparisons are listed below.

Approximation	Boundary points used	Average relative error	Computing time
Constant	24	7.83%	1.9 sec.
Biquadratic shape function	20	0.01%	3.4 sec.

(b) Consider a plate with a hole at the center and all the temperature distribution $u = \left(u_i - \frac{(u_i - u_o)}{\ln(r_i/r_o)} \ln r_i\right) + \left(\frac{u_i - u_o}{\ln(r_i/r_o)}\right) \ln r$

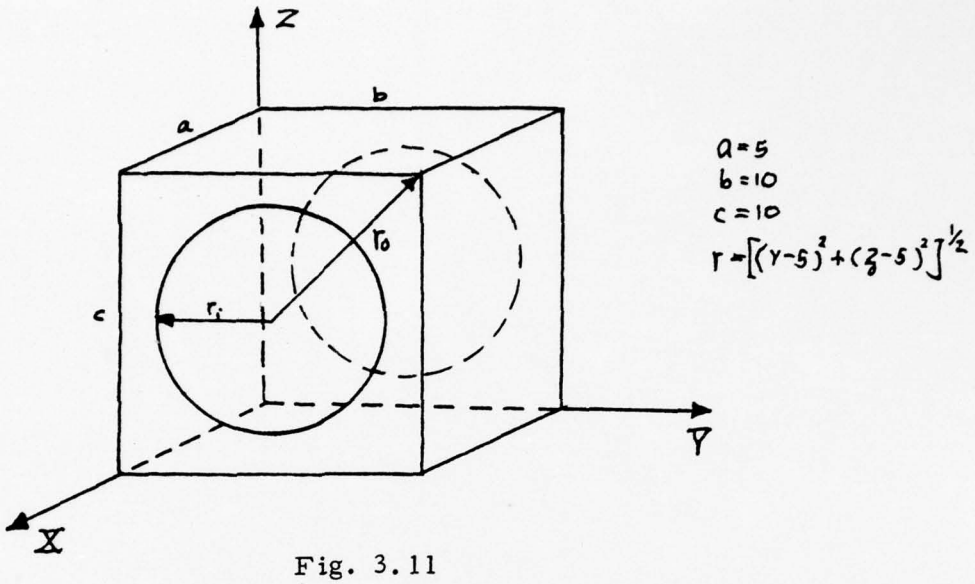

Fig. 3.11

After solving for the boundary heat flux by using BIE method with biqua-quadratic shape function approximation for different Gaussian points, 4 and 5, the comparisons are listed below:

Quadratic Shape Function Approximation

(120 Boundary points used)

Gaussian points used	Average relative error	Computing time
4	5.7%	4 4 sec.
5	1.2%	6 2 sec.

(c) Consider a solid sphere, as shown in Fig. 3.12, with the axisymmetrical surface temperature distribution $u(r_o, \theta) = \cos\theta$

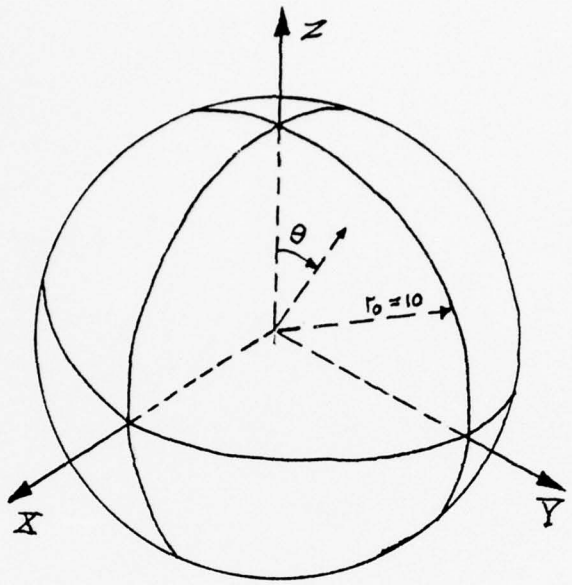

Fig. 3.12

The exact analytical solution is $u(r, \theta) = r/r_o \cos\theta$. It is desired to solve, by using quadratic shape function approximation, for the boundary heat flux, and then solve for some interior temperatures. Results are given in the following table:

Quadratic Shape Function Approximation
(32 boundary points used)
(4.5 sec. computing time)

Interior Coordinates			Analytical Solution	Numerical Solution	Relative Error
x	y	z			
7.0	7.0	0	0.0000	0.0000	
1.0	2.0	3.0	0.3000	0.2976	0.8%
4.0	4.0	4.0	0.4000	0.3948	1.3%
5.0	4.0	5.0	0.5000	0.5035	0.7%

CHAPTER FOUR

DISCUSSION AND CONCLUSION

The purpose of the work in this thesis is two-fold, viz.,

(1) to apply the BIE method to Laplacian problems:

(2) to supply various numerical approximations in dealing with such applications.

For the first purpose, it is obvious that the BIE method has a basic advantage over other numerical methods like the FDM and FEM, due to the reduction of dimension by one. Thus the efforts in the numerical modelling and preparing the geometrical data have been greatly decreased, especially when the ratio of the surface area to the volume of the domain concerned is relatively low. However, there are some drawbacks with the BIE, e.g.,

(1) it is applicable only to linear problems;

(2) the coefficient matrix involved, i.e., [A] and [B] shown in Chapter 2 and 3, is a full matrix, therefore not like the banded and sparse matrix involved in some other numerical methods, like FEM. This is an undesirable computational feature.

However, despite these drawbacks, the BIE is still worthy to be recommended as a useful numerical method to deal with boundary value problems.

As to the second purpose, it is clear that one can not say in advance which numerical approximation is superior to the others. The term

"improved" used in Chapter 3 simply means the following:

(1) Instead of the piecewise step function approximation, we introduce the higher degree, quadratic, piecewise interpolating polynomial to approximate the boundary function. From the error estimate it can be shown that, in general, the latter approximation will have better accuracy than the former with the same mesh. Also, by using the isoparametric transformation as explained in Chapter 3.1, this approximation method is made more useful.

(2) When considerable smoothness of the representation is necessary or desirable, we further introduce the spline function approximation. Here, unlike the former two approximations, continuity of the derivatives of the approximation function at the knots are also assured.

Besides these two facts, there are various other factors which must be taken into consideration in order to say which approximation method is improved or not. Specifically, consider the following:

(1) From the error analysis for the piecewise quadratic Lagrange's polynomial approximation [11], it is found that

$$\| f - p_2 \| \leq \frac{\| f''' \| h^3}{12}$$

where f is the function to be approximated, p_2 is the piecewise quadratic Lagrange's interpolating polynomial, and h is the mesh length interval between nodes. An error analysis for the cubic

spline function approximation [21] leads to

$$\| f - s_3 \| \leq \frac{5 \| f^{(4)} \| h^4}{384}$$

where s_3 is the cubic spline function. We can predict that the cubic spline function approximation will have the faster convergent speed as the mesh length h decreases.

(2) In order to achieve the same accuracy, the quadratic shape function approximation may require less computing time. This has been shown in the results of test problems.

(3) The effort spent on the programming is also taken into consideration. The piecewise constant approximation is relatively easy to deal with. In contrast, the shape function and spline function approximations are comparably complicated to program.

Therefore, whether a specific numerical approximation is "improved" or not to any analyst depends on the accuracy needed, computing time available, and programming efforts.

In Sec. 3.3, we have posed several test problem. From them, we can see the following:

(1) From the viewpoint of accuracy, shape function approximation is much better at the beginning, while

(2) From the viewpoint of convergence speed, spline function approximation is faster then the other two approximations;

(3) From the viewpoint of computing time, it is worth while to use step function approximation at first if the analyst wants a

rough idea about the solution field.

(4) Accuracy could also be improved by increasing the number of Gaussian points see (Appendix 2).

All of these programs were run on an IBM 370 Model 165 computer.

There are further considerations with the different approximations. When we use step function approximation, function values defined are those at the centroid of the segment, so we do not have the so-called "sharp-corner" problem, where the normal derivative of the potential function is discontinuous. However, in the shape function and spline function approximation, we do have the sharp-corner problem, because in these two approximations, function values are defined at the boundary points of the individual segment. To deal with this in shape function approximation, it should be remembered that only one unknown can be found at a nodal point. So if the potential function is an unknown, all the different values of its normal derivative should be defined; or if potential function is defined, then all but one of its normal derivatives still needs to be defined. The value of the normal derivative can be determined via the boundary geometry and the potential function distribution. Take a two-dimensional rectangle as an example, as shown in Fig. 4.1,

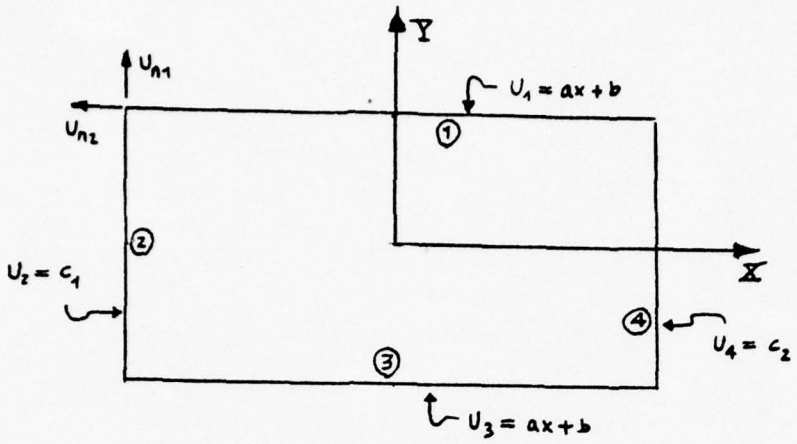

Fig. 4.1

where

$$u_{n_2} = \frac{du_2}{dn} = \frac{du_1}{dt} = a$$

$$u_{n_1} = \frac{du_1}{dn} = \frac{du_2}{dt} = 0$$

and t is the tangential direction.

As to the cubic spline function approximation, because of its inherent smoothness property, the function to be approximated should be continuous and have continuous first and second derivatives. Therefore, in dealing with the sharp corner problem, we should discard the periodic spline approximation, and instead we should use the ordinary spline which ends at these points where discontinuity occured.

There is another way to achieve the smoothness requirement, i.e., to consider the piecewise Hermitian polynomial, take the piecewise cubic Hermites, p(t), for example,

$$p(t) = \sum_{i=0}^{N} f(t_i)h_{i0}(t) + \sum_{i=0}^{N} f'(t_i)h_{i1}(t) \qquad (4.1)$$

where f(t) is the function to be approximated, and $h_{i0}(t)$, $h_{i1}(t)$ are those cubic Hermitian shape functions which, similar to the Lagrangian shape function, Eq. (3.2), have the following properties:

$$h_{i0}(t_j) = \delta_{ij}$$

$$h'_{i0}(t_j) = 0$$

$$h_{i1}(t_j) = 0$$

$$h'_{i1}(t_j) = \delta_{ij}$$

Thus p(t) has the continuity of the first derivative of f(t). Substituting Eq. (4.1) into the two-dimensional boundary-boundary integral equation and interior-boundary integral equation, we can solve the problem by procedures similar to those described in Sec. 3.1.A., with the isoparametric transformation. However, the difficulties are two-fold.

(1) It is not always possible to obtain accurate values for the derivatives of the known function.

(2) Because the number of the known and unknown functions has been doubled, the size of the resulted coefficient matrix, [A] and [B], have been enlarged from N x N to 2N x 2N, where N is the number of the points where either u or u_n has been defined.

Therefore, we did not consider the Hermite Polynomial method in this

thesis, but, if necessary, it can be implemented readily.

Finally, as is pointed out in the beginning of this chapter, there is no absolute advantage of any numerical approximation. Therefore, trying to find a "better" approximation in order to improve the efficiency of the BIE method is frequently necessary. Also, it is possible to generalize the methods mentioned in this thesis to the boundary value problems governed by other differential equations, e.g., Poisson's equation, and equations which govern inhomogeneous media such as bodies with inclusions where conditions of continuity at the interface boundaries need be considered.

APPENDIX I

CALCULATION OF ELEMENTS OF COEFFICIENT MATRIX IN PIECEWISE STEP FUNCTION APPROXIMATION

1.1 Two-Dimensional Case:

1.1.1 Calculation of a_{ij}:

$$a_{ij} = \int_{B_j} \frac{\partial \log r(p_i, q)}{\partial n} ds(q) - \delta_{ij} \sum_{k=1}^{N} \int_{B_k} \frac{\partial \log r(p_i, q)}{\partial n} ds(q) \quad (2.24)$$

The typical part of right hand side of Eq. (2.24) is

$$\int_{B_j} \frac{\partial \log r(p_i, q)}{\partial n} ds(q)$$

for which we have two different conditions, $i \neq j$ and $i = j$:

(i) $i \neq j$

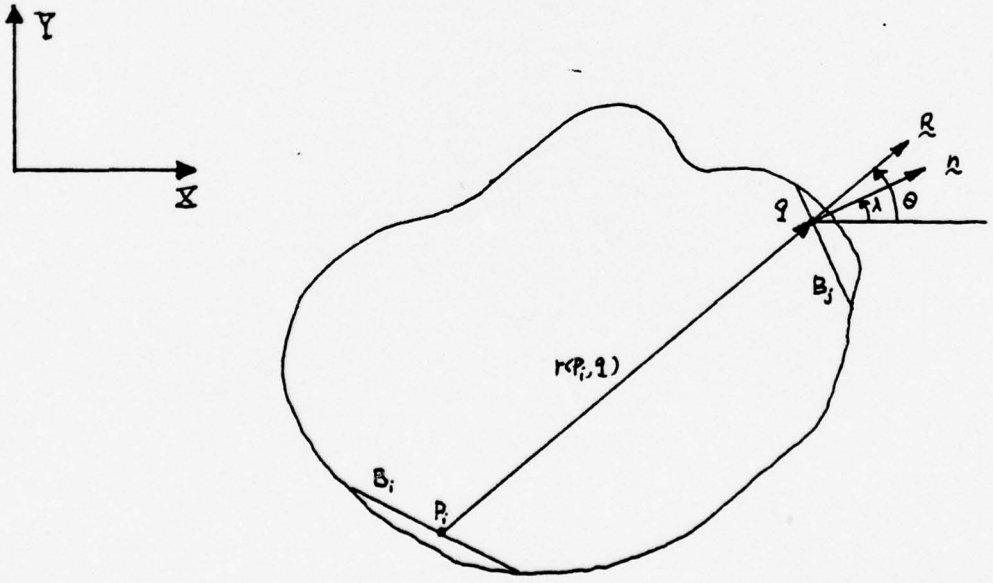

Fig. A.1.1

$$\frac{\partial \log r(p_i, q)}{\partial n} = \frac{\partial \log r}{\partial x} \frac{\partial x}{\partial n} + \frac{\partial \log r}{\partial y} \frac{\partial y}{\partial n}$$

$$= \frac{1}{r} (\cos\theta\cos\lambda + \sin\theta\sin\lambda$$

$$= \frac{1}{r} \cos(\theta - \lambda)$$

$$= \frac{d\theta}{ds}$$

where the angles are as shown in Fig. A.1.1.

Thus,

$$a_{ij} = \int_{B_j} d\theta_i = \theta_{ij}$$

(ii) $i = j$

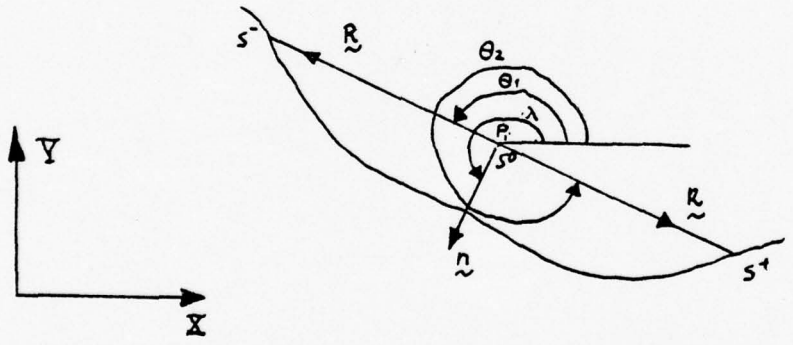

Fig. A.1.2

$$\int_{B_i} \frac{\partial \log r(p_i, q)}{\partial n} ds(q) = \int_{s^-}^{s^0 - \epsilon'} \frac{\partial \log r(p_i, q)}{\partial n} ds(q) +$$

$$+ \int_{s^0 - \epsilon'}^{s^0 + \epsilon''} \frac{\partial \log r(p_i, q)}{\partial n} ds(q) + \int_{s^0 + \epsilon''}^{s^+} \frac{\partial \log r(p_i, q)}{\partial n}$$

since

$$\lim_{\epsilon' \to 0} \int_{s^-}^{s^0-\epsilon'} \frac{\partial \log r(p_i, q)}{\partial n} ds(q) = \lim_{\epsilon' \to 0} \int_{s^-}^{s^0-\epsilon'} \frac{1}{r} \cos(\theta_1 - \lambda) ds(q) = 0$$

$$\lim_{\epsilon'' \to 0} \int_{s^0+\epsilon''}^{s^+} \frac{\partial \log r(p_i, q)}{\partial n} ds(q) = \lim_{\epsilon'' \to 0} \int_{s^0+\epsilon''}^{s^+} \frac{1}{r} \cos(\lambda - \theta_2) ds(q) = 0$$

where the angles in the expressions above are as shown in Fig. A.1.2. The sum of these two integrals always has a limit, i.e., 0, no matter how the ϵ' and ϵ'' tend to zero independently of each other. Thus, by the definition of the improper integral, we know that

$$\int_{B_i} \frac{\partial \log r(p_i, q)}{\partial n} ds(q) = \lim_{\substack{\epsilon' \to 0 \\ \epsilon'' \to 0}} \left(\int_{s^-}^{s^0-\epsilon'} \frac{\partial \log r(p_i, q)}{\partial n} ds(q) + \int_{s^0+\epsilon''}^{s^+} \frac{\partial \log r(p_i, q)}{\partial n} ds(q) \right)$$

$$= 0$$

Therefore,

$$a_{ij} = -\delta_{ii} \sum_{\substack{k=1 \\ k \neq i}}^{N} \theta_{ik} = -\pi$$

1.1.2 Calculation of b_{ij}:

$$b_{ij} = \int_{B_j} \log r(p_i, q) ds(q) \qquad (2.25)$$

Again there are two different conditions, $i \neq j$ and $i = j$:

(i) $i \neq j$

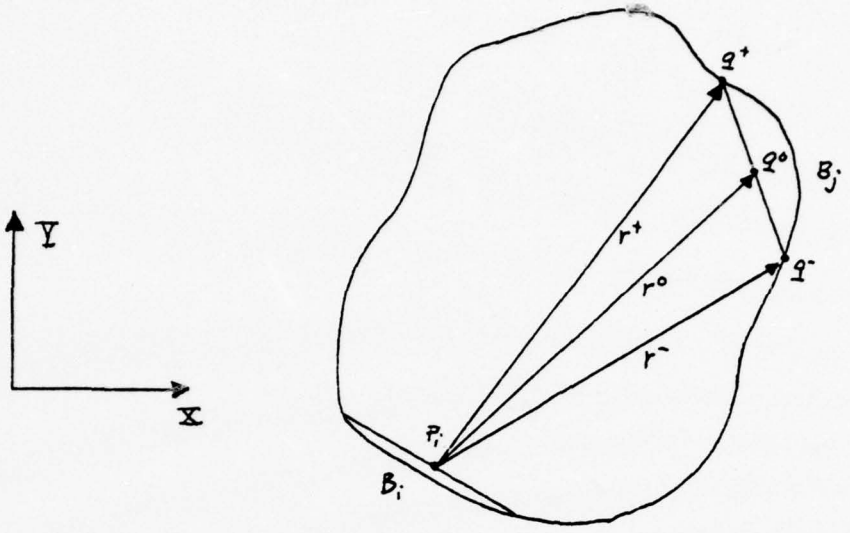

Fig. A.1.3

There are various ways to calculate this nonsingular integral numerically. We adopt Simpson's rule:

$$b_{ij} = \frac{\Delta s_i}{6}\left[\log r(p_i, q^-) + 4\log r(p_i, q^0) + \log r(p_i, q^+)\right]$$

cf. Fig. A.1.3.

(ii) i = j

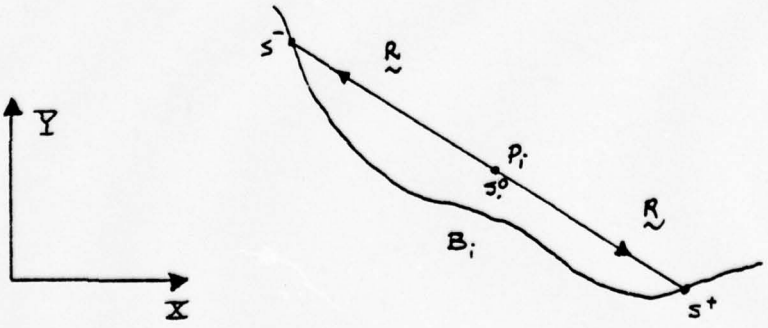

Fig. A.1.4

$$b_{ii} = \lim_{s \to s^0} \int_{s^-}^{s} \log r(p_i, q) ds(q) + \lim_{s \to s^0} \int_{s}^{s^+} \log r(p_i, q) ds(q)$$

$$= \lim_{r \to 0} \int_{r^-}^{r} \log r(p_i, q)(-dr(q)) + \lim_{r \to 0} \int_{r}^{r^+} \log r(p_i, q) dr(q)$$

$$= 2 \lim_{r \to 0} \int_{r}^{r^+} \log r(p_i, q) dr(q)$$

$$= 2 \lim_{r \to 0} [r(p_i, q) \log r(p_i, q) - r(p_i, q)]_{r}^{r^+}$$

$$= 2[r^+ \log r^+ - r^+ - \lim_{r \to 0}(r \log r - r)]$$

$$= 2\, r^+(\log r^+ - 1)$$

$$= \Delta s_i [\log \left(\frac{\Delta s_i}{2} \right) - 1]$$

cf. Fig. A.1.4.

1.1.3. Calculation of k_{1i} and k_{2i}:

$$k_{1i} = \int_{B_i} \frac{\partial \log r(t, q)}{\partial n} ds(q) \qquad (2.31)$$

$$k_{2i} = \int_{B_i} \log r(t, q) ds(q) \qquad (2.32)$$

Since t is not on the boundary, there is no singular case and we can write the expression for k_{1i} and k_{2i} directly from A.1.1.1 (i) and A.1.1.2(i), respectively, i.e.,

$$k_{1i} = \Delta\theta_{ti}$$

$$k_{2i} = \frac{\Delta s_i}{6} \left[\log r(t,q^-) + 4\log r(t,q^0) + \log r(t,q^+)\right]$$

See Fig. A.1.5.

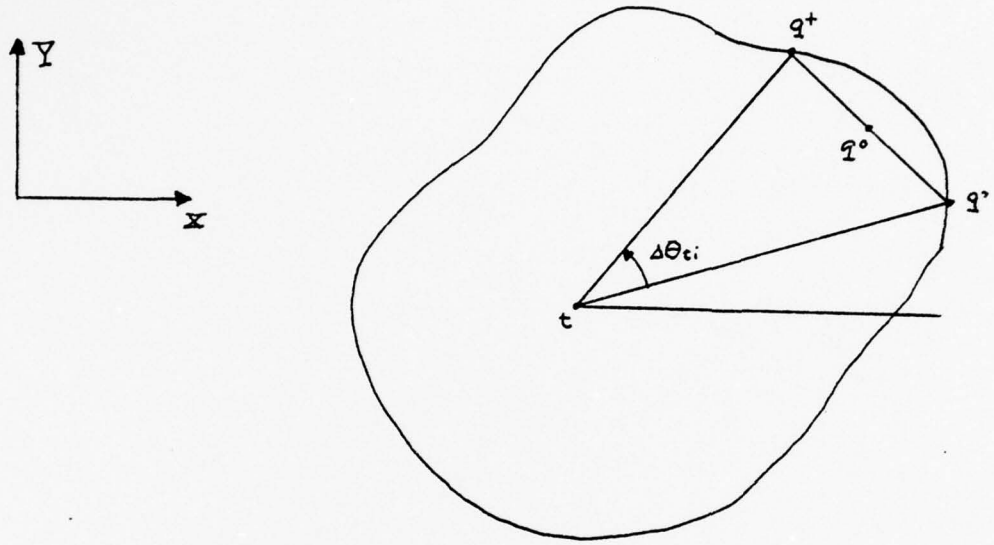

Fig. A.1.5

1.2 Three-Dimensional Case:

1.2.1 Calculation of a_{ij}:

$$a_{ij} = \int_{B_j} \frac{\partial}{\partial n} \frac{1}{r(p_i,q)}\, da(q) - \delta_{ij} \sum_{k=1}^{N} \int_{B_k} \frac{\partial}{\partial n} \frac{1}{r(p_i,q)}\, da(q) \qquad (2.36)$$

The typical part of the right-hand side of Eq. (2.36) is

$$\int_{B_i} \frac{\partial}{\partial n} \frac{1}{r(p_i,q)}\, da(q)$$

As before, we consider the $i \neq j$ and $i = j$ conditions separately:

(i) $i \neq j$

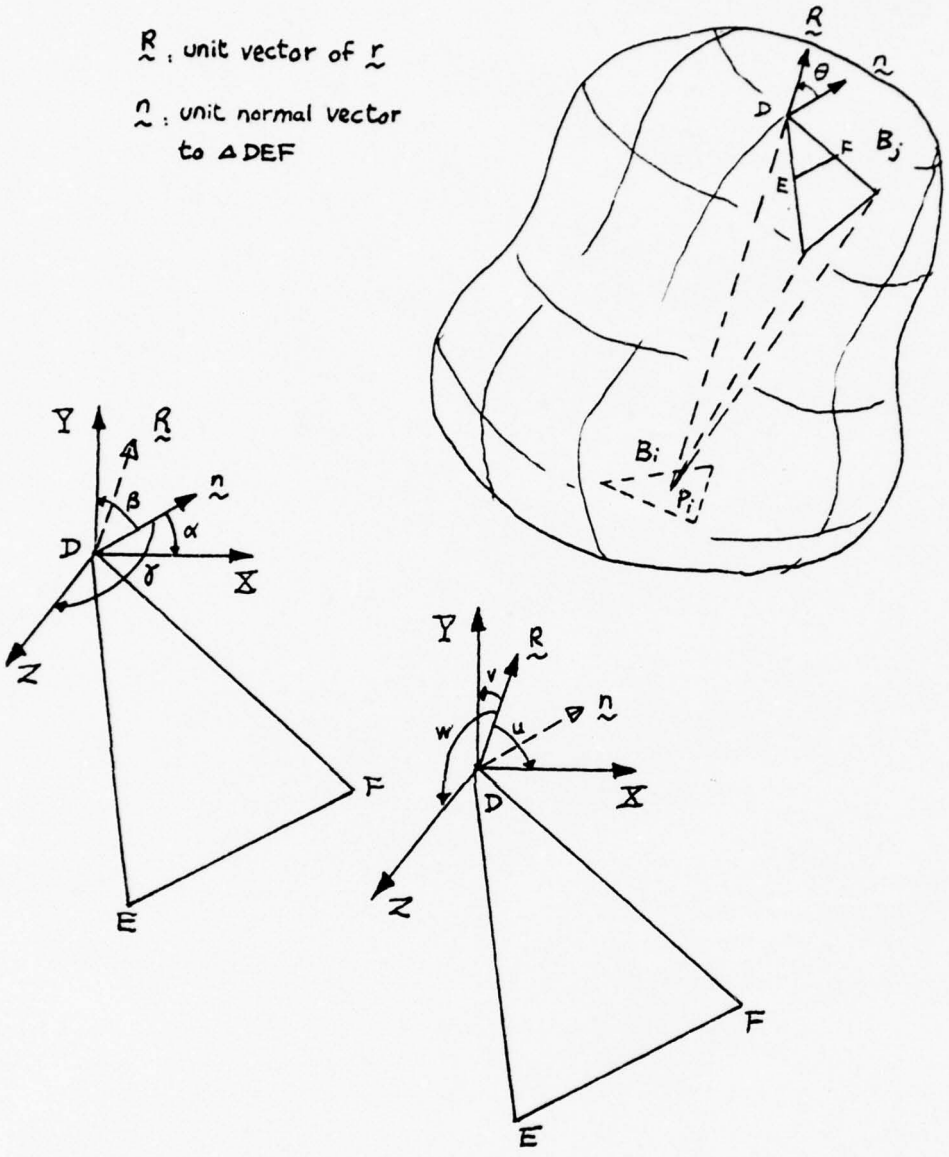

Fig. A.1.6

$$\frac{\partial}{\partial n}\ \frac{1}{r(p_i,q)} = \frac{\partial}{\partial x}\ \frac{1}{r(p_i,q)}\ \frac{\partial x}{\partial n} + \frac{\partial}{\partial y}\ \frac{1}{r(p_i,q)}\ \frac{\partial y}{\partial n} + \frac{\partial}{\partial z}\ \frac{1}{r(p_i,q)}\ \frac{\partial z}{\partial n}$$

$$\frac{\partial}{\partial n}\frac{1}{r(p_i,q)} = -\frac{1}{r^2}(\cos u \cos\alpha + \cos v \cos\beta + \cos w \cos\gamma)$$

$$= -\frac{1}{r^2}(\underset{\sim}{R}\cdot\underset{\sim}{n})$$

$$= -\frac{1}{r^2}\cos\theta.$$

See Fig. A.1.6.

However, it has been noted that

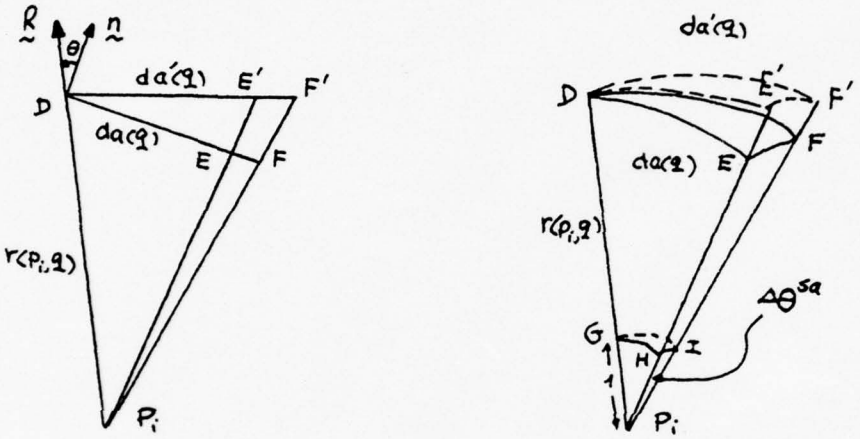

Fig. A.1.7

$$\cos\theta = \frac{da'(q)}{da(q)}$$

and

$$\frac{1}{r^2} = \frac{d\theta^{sa}}{da'(q)}$$

where $da'(q)$ is a segment surface of the sphere with radius r, centered at p_i, and $d\theta^{sa}$ is the solid angle confined by the cone p_iDEF, See Fig. A.1.7. Thus

$$\frac{\partial}{\partial n}\,\frac{1}{r(p_i, q)} \;=\; -\,\frac{d\theta^{sa}}{da(q)}$$

and therefore

$$a_{ij} = -\int_{B_j} d\theta_i^{sa}$$

$$= -\,\Delta\theta_{ij}^{sa}$$

where

$\Delta\theta^{sa}$ = area of GHI

$$= 4\tan^{-1}\sqrt{\tan\tfrac{1}{2}s\cdot\tan\tfrac{1}{2}(s-a)\cdot\tan\tfrac{1}{2}(s-b)\cdot\tan\tfrac{1}{2}(s-c)}$$

$a = \angle\, Gp_iH$

$b = \angle\, Hp_iI$

$c = \angle\, Ip_i0$

$s = \frac{a+b+c}{2}$

(ii) i = j

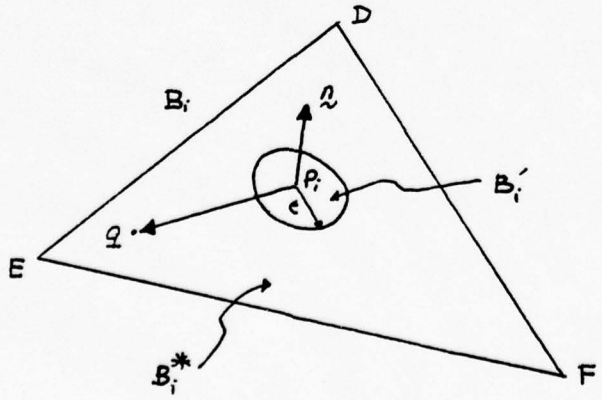

Fig. A.1.8

It can be seen from Fig. A.1.8 that

$$\int_{B_i} \frac{\partial}{\partial n} \frac{1}{r(p_i,q)} \, da(q) = \int_{B_i^*} \frac{\partial}{\partial n} \frac{1}{r(p_i,q)} \, da(q)$$

$$+ \int_{B_i'} \frac{\partial}{\partial n} \frac{1}{r(p_i,q)} \, da(q)$$

and

$$\int_{B_i^*} \frac{\partial}{\partial n} \frac{1}{r(p_i,q)} \, da(q) = \int_{B_i^*} - \frac{1}{r^2} (\underline{R} \cdot \underline{n}) da(q) = 0$$

That is to say, no matter how ϵ approaches zero, the integral over this plane triangle without the circular area with radius ϵ and center p_i will always have the same limit, 0. Thus from the definition of an improper integral we know then

$$\int_{B_i} \frac{\partial}{\partial n} \frac{1}{r(p_i,q)} \, da(q) = \lim_{\epsilon \to 0} \int_{B_i^*} \frac{\partial}{\partial n} \frac{1}{r(p_i,q)} \, da(q) = 0$$

Therefore, we know that

$$a_{ii} = - \delta_{ii} \sum_{\substack{k=1 \\ k \neq i}}^{N} \Delta\theta_{ik}^{sa}$$

$$= 2\pi$$

1.2.2 Calculation of b_{ij}:

$$b_{ij} = \int_{B_j} \frac{1}{r(p_i,q)} \, da(q) \qquad (2.37)$$

(i) $i \neq j$

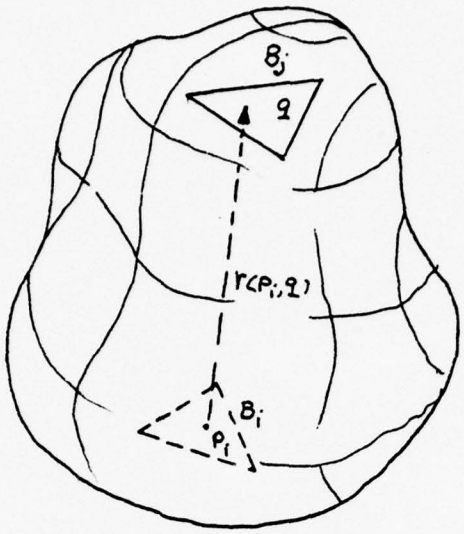

Fig. A.1.9

In spite of considerable recent activity in the field of methods for evaluating multiple integrals, the general theory is relatively undeveloped. The method used here for the approximate integrals of functions over a triangle (cf. Fig. A.1.9) is the 64-point, 15th degree triangular, product Gauss formula [18].

(ii) $i = j$

Taking a right triangle into consideration, (Fig. A.1.10) we know that

Fig. A.1.10

$$\int_{rt.\Delta} \frac{1}{r}\, da = \int_0^{x_1} \int_0^{x\tan\theta_1} \frac{1}{\sqrt{x^2 + y^2}}\, dy dx$$

$$= \int_0^{x_1} \log(y + \sqrt{x^2 + y^2})_0^{x\tan\theta_1} dx$$

$$= \log[\tan\theta_1 + \sec\theta_1] \int_0^{x_1} dx$$

$$= s\log(\tan\theta_1 + \sec\theta_1)$$

Thus, for an arbitrary triangle (Fig. A.1.11)

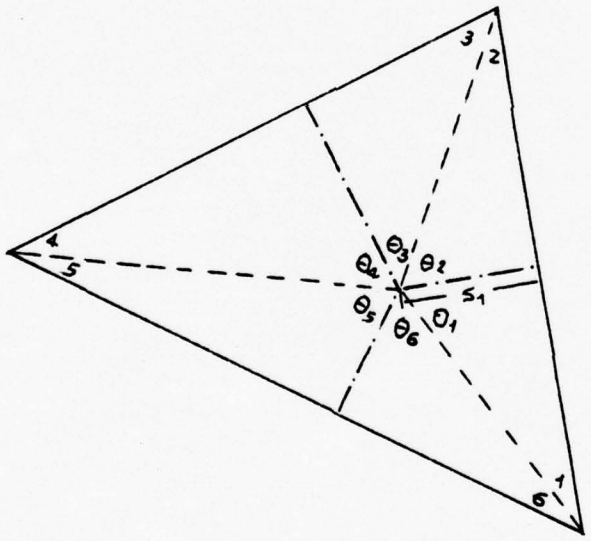

Fig. A.1.11

$$b_{ii} = \int_{B_i} \frac{1}{r(p_i, q)}\, da(q)$$

$$= \sum_{k=1}^{6} \int_{rt \cdot \Delta} \frac{1}{r(p_i, q)}\, da(q)$$

$$= \sum_{k=1}^{6} s_k \log(\tan\theta_k + \sec\theta_k)$$

where

$$s_{2k-1} = s_{2k} \qquad k = 1, 2, 3$$

1.2.3 Calculation of k_{1i} and k_{2i}:

$$k_{1i} = \int_{B_i} \frac{\partial}{\partial n} \frac{1}{r(t, q)}\, da(q) \tag{2.39}$$

$$k_{2i} = \int_{B_i} \frac{1}{r(t, q)}\, da(q) \tag{2.40}$$

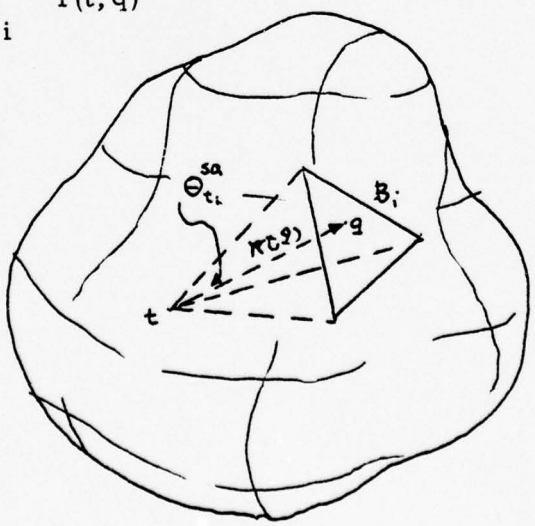

Fig. A.1.12

Since t is not on the boundary, (cf. Fig. A.1.12) there is no singular case, and we can write the expression for k_{1i} directly from A.1.2.1 (i).

$$k_{1i} = - \Delta\theta^{sa}_{t_i}$$

and calculate k_{2i} by the 64-point, 15 degree triangular-product Gauss formula as in A.1.2.2(i).

APPENDIX II

CALCULATION OF ELEMENTS OF COEFFICIENT MATRIX IN QUADRATIC SHAPE FUNCTION APPROXIMATION

2.1 Two-Dimensional Case:

2.1.1 Calculation of a_{ii}^{α} and a'_{ij}:

$$a_{ij}^{\alpha} = \int_{-1}^{1} N^{\alpha}(e) \frac{\partial \log r(p_i, q_j(e))}{\partial n} J(e)de$$

$$a'_{ij} = \int_{-1}^{1} \frac{\partial \log r(p_i, q_j(e))}{\partial n} J(e)de$$

As in the previous Appendix, we will have two cases to be considered. (i) p_i is not situated within the j^{th} segment, (neither on the end point nor on the midpoint of the j^{th} segment, (cf. Fig. A.2.1).

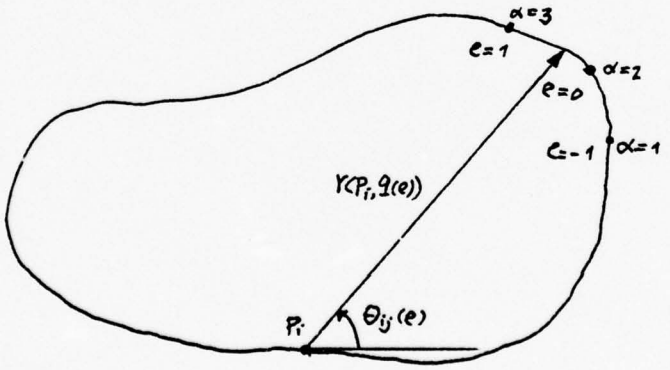

Fig. A.2.1

According to A.1.1.1 (i), we know that

$$\frac{\partial \log r(p_i, q)}{\partial n} = \frac{d\theta}{ds}$$

Therefore, a_{ij}^{α} , a'_{ij} can be rewritten as

$$a_{ij}^{\alpha} = \int_{-1}^{1} N^{\alpha}(e) \frac{d\theta_{ij}(e)}{de} de$$

$$a'_{ij} = \int_{-1}^{1} \frac{d\theta_{ij}(e)}{de} de$$

and

$$\theta_{ij}(e) = \tan^{-1} \frac{(y_j(e) - y(p_i))}{(x_j(e) - x(p_i))}$$

$$\frac{d\theta_{ij}(e)}{de} = \frac{y_j'(e)(x_j(e) - x(p_i)) - x_j'(e)(y_j(e) - y(p_i))}{(x_j(e) - x(p_i))^2 + (y_j(e) - y(p_i))^2}$$

Let

$$F_{ij}^{\alpha}(e) = N^{\alpha}(e) \frac{d\theta_{ij}(e)}{de}$$

$$G_{ij}(e) = \frac{d\theta_{ij}(e)}{de}$$

we can thus use the m-point Gaussian quadrature formula [19] to calculate the integrand numerically as

$$a_{ij}^{\alpha} = \sum_{k=1}^{m} w_k F_{ij}^{\alpha}(e_k)$$

$$a'_{ij} = \sum_{k=1}^{m} w_k G_{ij}(e_k)$$

where w_k is the weight function.

(ii) p_i is situated within j^{th} segment, (cf. Fig. A.2.2).

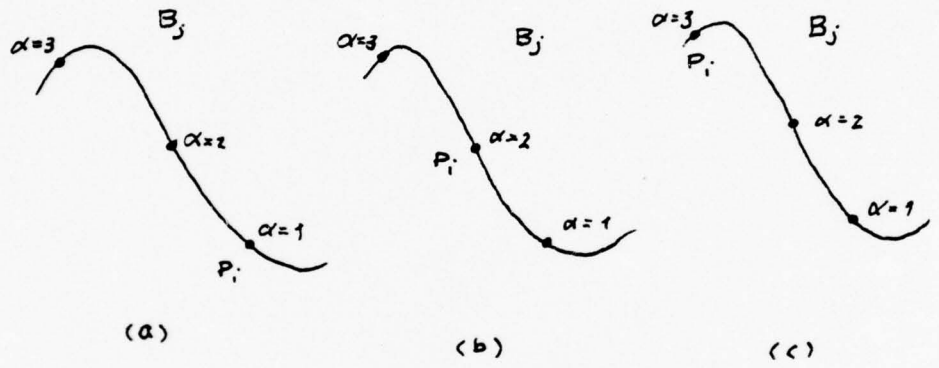

Fig. A.2.2.

Let

$$\bar{a}_{ij}^{\alpha} = a_{ij}^{\alpha} - \delta_{ij}(\alpha) a'_{ij}$$

$$= \int_{-1}^{1} (N^{\alpha}(e) - \delta_{ij}(\alpha)) \frac{d\theta_{ij}(e)}{de} de$$

$$\lim_{q_j(e) \to p_i} (N^{\alpha}(e) - \delta_{ij}(\alpha)) \frac{d\theta_{ij}(e)}{de} =$$

$$\lim_{q_j(e)\to p_i} \frac{(N^{\alpha}(e) - \delta_{ij}(\alpha))(y_j'(e)(x_j(e) - x(p_i)) - x_j'(e)(y_j(e) - y(p_i)))}{(x_j(e) - x(p_i))^2 + (y_j(e) - y(p_i))^2}$$

$$= \frac{0}{0}$$

which is an indeterminate form. However, by using l'Hopital's rule twice, we found that

$$\lim_{q_i(e)\to p_i} (N^{\alpha}(e) - \delta_{ij}(\alpha)) \frac{d\theta_{ij}(e)}{de} =$$

$$\frac{(N^{\alpha}(e))''(y_j'(e)(x_j(e) - x(p_i)) - x_j'(e)(y_j(e) - y(p_i)))}{D}$$

$$+ \frac{2(N^{\alpha}(e))'(y_j''(e)(x_j(e) - x(p_i)) - x_j''(e)(y_j(e) - y(p_i)))}{D}$$

$$+ \frac{(N^{\alpha}(e) - \delta_{ij}(\alpha))(y_j''(e)x_j'(e) - x_j''(e)y_j'(e))}{D} = 0$$

$$D = 2((x_j(e) - x(p_i))x_j''(e) + (x_j'(e))^2 + (y_j(e) - y(p_i))y''(e) + (y'(e))^2)$$

Therefore, we know in fact that there is no singularity, so that we can calculate $\bar{a}_{ij}^{\alpha}$ as we did in A.2.1.1 (j); i.e., let

$$\bar{F}_{ij}^{\alpha}(e) = (N^{\alpha}(e) - \delta_{ij}(\alpha)) \frac{d\theta_{ij}(e)}{de}$$

and

$$\bar{a}_{ij}^{\alpha} = \sum_{k=1}^{m} w_k \bar{F}_{ij}^{\alpha}(e_k)$$

2.1.2 Calculation of b_{ij}^{α}:

$$b_{ij}^{\alpha} = \int_{-1}^{1} N^{\alpha}(e)\log r(p_i, q_j(e))J(e)de$$

As before, we have two different conditions to be handled.

(i) p_i is not situated within j^{th} segment as shown in Fig. A.2.1. There is no possibility to have a singularity; therefore let

$$H_{ij}^{\alpha}(e) = N^{\alpha}(e)\log r(p_i, q_j(e))J(e)$$

and using the m-point Gaussian quadrature formula, we have

$$b_{ij}^{\alpha} = \sum_{k=1}^{m} w_k H_{ij}^{\alpha}(l_k)$$

(ii) p_i is situated within j^{th} segment as shown in Fig. A.2.2:

$$b_{ij}^{\alpha} = \int_{-1}^{1} N^{\alpha}(e)\log r(p_i, q_j(e))J(e)de$$

We have three cases to discuss:

(a) Let $j(1) = i$, as shown in Fig. A.2.2 (a)

$$b_{ij} = \int_{-1}^{0} N^{\alpha}(e)\log r(p_i, q_j(e))J(e)de + \int_{0}^{1} N^{\alpha}(e)\log r(p_i, q_j(e))J(e)de$$

The second part of the right-hand side is free of singularity, so we treat it as in A.2.1.2 (i); i.e., let

$$H_{ij}^{\alpha}(e) = N^{\alpha}(e)\log r(p_i, q_j(e))J(e)$$

As to the first part, we let

$$e = f^2 - 1$$

thus, $de = 2\,f\,df$

$$\int_{-1}^{0} N^{\alpha}(e)\log r(p_i, q_j(e))J(e)de = \int_{-1}^{0} N^{\alpha}(e(f))\log r(p_i, q_j(e(f))J(e(f))(-2f)df$$

where

$$\lim_{q_i(f)\to p_i} \log r(p_i, q_j(e(f))) \cdot df = \lim_{f\to 0} \log f \cdot f = 0$$

while $N^{\alpha}(e(f))$ and $J(e(f))$ are finite within the range $f \in (-1, 0)$; therefore we can let

$$\bar{H}_{ij}^{\alpha}(f) = N^{\alpha}(e(f))\log r(p_i, q_j(e(f)))J(e(f))(-2f)$$

and use the m-point Gaussian quadrature formula

$$b_{ij}^{\alpha} = \sum_{k=1}^{m} w_k(\bar{H}_{ij}^{\alpha}(f_k) + H_{ij}^{\alpha}(e_k))$$

where $f \in (-1, 0)$ and $e \in (0, 1)$.

Similarly, we can use the following expression for the other two cases:

(b) $j(2) = i$, as shown in Fig. A.2.2 (b).

Let

$$-e = f^2 \qquad \text{for } e \in (-1, 0)$$

$$e = g^2 \qquad \text{for } e \in (0, 1)$$

therefore

$$b_{ij}^{\alpha} = \int_{-1}^{0} N^{\alpha}(e(f))\log\, r(p_i, q_j(e(f)))J(e(f))(-2f)df$$

$$+ \int_{0}^{1} N^{\alpha}(e(g))\log\, r(p_i, q_j(e(g)))J(e(g))(2g)dg$$

and let

$$\bar{H}_{ij}^{\alpha}(f) = N^{\alpha}(e(f))\log\, r(p_i, q_j(e(f)))J(e(f))(-2f)$$

$$\bar{\bar{H}}_{ij}^{\alpha}(g) = -\bar{H}_{ij}^{\alpha}(g)$$

Thus

$$b_{ij}^{\alpha} = \sum_{k=1}^{m} w_k (\bar{H}_{ij}^{\alpha}(f_k) + \bar{\bar{H}}_{ij}^{\alpha}(g_k))$$

where $f \in (-1, 0)$ and $g \in (0, 1)$.

(c) $j(3) = i$, as shown in Fig. A.2.2 (c).

Let

$$-e = g^2 - 1 \qquad \text{for } e \in (0, 1)$$

therefore

$$b_{ij} = \int_{-1}^{0} N^{\alpha}(e)\log\, r(p_i, q_j(e))J(e)de$$

$$+ \int_{0}^{1} N^{\alpha}(e(g))\log\, r(p_i, q_j(e(g))J(e(g))(2g)dg$$

and let

$$H_{ij}^{\alpha} = N^{\alpha}(e)\log\, r(p_i, q_j(e))J(e)$$

$$\bar{\bar{H}}_{ij}^{\alpha} = N^{\alpha}(e(g))\log\, r(p_i, q_j(e(g)))J(e(g))(2g)$$

Thus

$$b_{ij}^{\alpha} = \sum_{k=1}^{m} w_k(H_{ij}^{\alpha}(e_k) + \bar{\bar{H}}_{ij}^{\alpha}(g_k))$$

where $e \in (-1, 0)$ and $g \in (0, 1)$.

2.1.3 Calculation of k_{1j}^{α} and k_{2j}^{α}:

$$k_{1j}^{\alpha} = \int_{-1}^{1} N^{\alpha}(e) \frac{\partial \log\, r(t, q_j(e))}{\partial n} J(e)de \qquad (3.13)$$

$$k_{2j} = \int_{-1}^{1} N^{\alpha}(e)\log\, r(t, q(e))J(e)de \qquad (3.14)$$

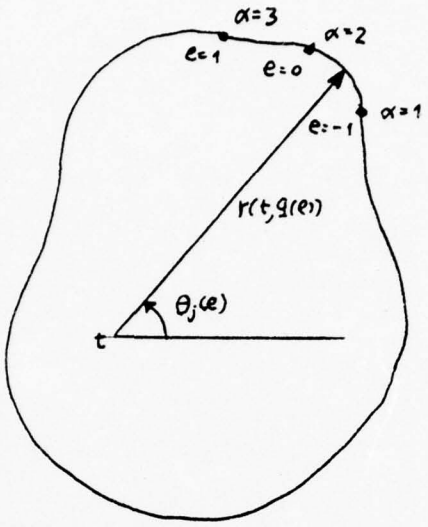

Fig. A.2.3

Since t is an interior point, (cf. Fig. A.2.3) there is no singular case and we can thus calculate k_{1j}^{α}, k_{2j}^{α} by using an m-point Gaussian quadrature formula, similar to the procedure described in A.2.1.1 (i) and A.2.1.2 (i):

$$k_{1j}^{\alpha} = \sum_{k=1}^{m} w_k F_j^{\alpha}(e_k)$$

$$k_{2j}^{\alpha} = \sum_{k=1}^{m} w_k H_j^{\alpha}(e_k)$$

where

$$F_j^{\alpha}(e) = N^{\alpha}(e) \frac{d\theta_j(e)}{de}$$

$$H_j^{\alpha}(e) = N^{\alpha}(e) \log r(t, q_j(e)) J(e)$$

and

$$\frac{d\theta_j(e)}{de} = \frac{y_j'(e)(x_j(e) - x(t)) - x_j'(e)(y_j(e) - y(t))}{(x_j(e) - x(t))^2 + (y_j(e) - y(t))^2}$$

2.2 Three-Dimensional Case:

2.2.1 Derivation of the parametric representation of boundary surface: Since a surface can be represented in parametric form by

$$\underline{r}(e,f) = x(e,f)\underline{i} + y(e,f)\underline{j} + z(e,f)\underline{k}$$

where $\underline{r}(e,f)$ is a vector function of two independent real variables, e and f, the so-called parameters or curvilinear coordinates, and is single-valued and continuous in a simply-connected bounded region of the e-f plane. It is found [20] that

$$da(q(e,f)) = J(e,f)de\ df$$

where

$$J(e,f) = \sqrt{EG - F^2}$$

$$E = \underline{r}e \cdot \underline{r}e$$

$$F = \underline{r}e \cdot \underline{r}f$$

$$G = \underline{r}f \cdot \underline{r}f$$

Thus

$$J(e,f) = \sqrt{(y_e z_f - y_f z_e)^2 + (x_e z_f - x_f z_e)^2 + (x_e y_f - x_f y_e)^2}$$

$$= \sqrt{N_1^{*2} + N_2^{*2} + N_3^{*2}}$$

The unit normal vector of surface concerned, $\underline{n}$ can be expressed as

$$\underline{n} = \frac{\underline{r}_e \times \underline{r}_f}{|\underline{r}_e \times \underline{r}_f|}$$

$$= \frac{N_1^*}{J(e,f)}\,\underline{i} + \frac{N_2^*}{J(e,f)}\,\underline{j} + \frac{N_3^*}{J(e,f)}\,\underline{k}$$

$$= n_x\underline{i} + n_y\underline{j} + n_z\underline{k}$$

2.2.2 Calculation of a_{ij}^{α} and a'_{ij}:

$$a_{ij}^{\alpha} = \int_{-1}^{1}\int_{-1}^{1} N^{\alpha}(e,f)\,\frac{\partial}{\partial n}\,\frac{1}{r(p_i, q_j(e,f))}\,J(e,f)\,de\,df$$

$$a'_{ij} = \int_{-1}^{1}\int_{-1}^{1} \frac{\partial}{\partial n}\,\frac{1}{r(p_i, q_i(e,f))}\,J(e,f)\,de\,df$$

The two different cases we considered are, (i) p_i is not situated within the j^{th} segment, as in Fig. A.2.4.

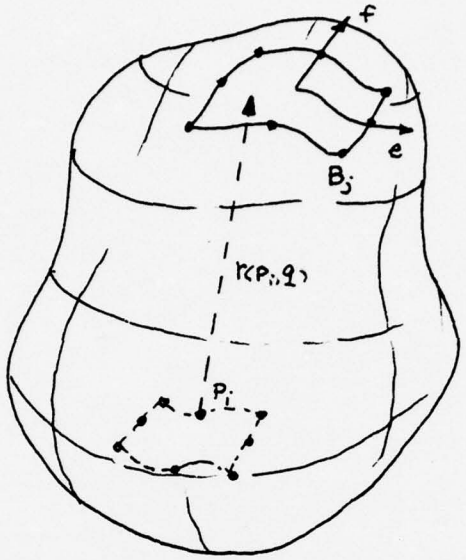

Fig. A.2.4

$$\frac{\partial}{\partial n}\ \frac{1}{r(p_i, q_j(e,f))} = -\ \frac{1}{r^2(p_i, q_j(e,f))}\ \frac{\partial r(p_i, q_j(e,f))}{\partial n}$$

$$= -\ \frac{1}{r(p_i, q_j(e,f))}\left[(x_j(q(e,f)) - x(p_i))n_x\right.$$

$$\left. + (y_j(q(e,f)) - y(p_i))n_y + (z_j(g(e,f)) - z(p_i))n_z\right]$$

Let

$$F_{ij}^{\alpha}(e,f) = N^{\alpha}(e,f)\ \frac{\partial}{\partial n}\ \frac{1}{r(p_i, q_j(e,f))} J(e,f)$$

$$G_{ij}(e,f) = \frac{\partial}{\partial n}\ \frac{1}{r(p_i, q_j(e,f))} J(e,f)$$

We can thus use (m1 x m2)-point Gaussian quadratic formula to calculate

$$a_{ij}^{\alpha},\ a'_{ij} \quad \text{as}$$

$$a_{ij}^{\alpha} = \sum_{k=1}^{m1} w_k \sum_{l=1}^{m2} w_l F_{ij}^{\alpha}(e_k, f_l)$$

$$a'_{ij} = \sum_{k=1}^{m1} w_k \sum_{l=1}^{m2} w_l G_{ij}(e_k, f_l)$$

(ii) p_i is situated within the j^{th} segment, i.e., to be one of the nodes of the j^{th} segment, either corner points, or midpoints as shown in Fig. A.2.5.

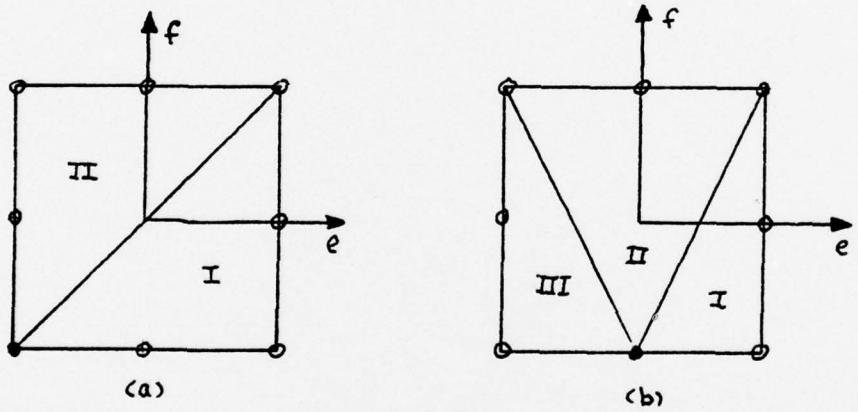

Fig. A.2.5

Let

$$a_{ij}^{-\alpha} = a_{ij}^{\alpha} - a'_{ij}$$

$$= \int_{-1}^{1}\int_{-1}^{1} (N^{\alpha}(e,f) - \delta_{ij(\alpha)}) \quad \frac{\partial}{\partial n} \quad \frac{1}{r(p_i, q_i(e,f))} \; J(e,f)\,de\,df$$

$$\bar{a}^{\alpha}_{ij} = \int_{-1}^{1}\int_{-1}^{1} (N^{\alpha}(e,f) - \delta_{ij(\alpha)}) \left[- \frac{Dx_{ij} N_1^* + Dy_{ij} N_2^* + Dz_{ij} N_3^*}{r^3(p_i, q_j(e,f))} \right] de\, df$$

where

$$Dx_{ij} = x_j(q(e,f)) - x(p_i)$$

$$Dy_{ij} = y_j(q(e,f)) - y(p_i)$$

$$Dz_{ij} = z_j(q(e,f)) - z(p_i)$$

The two typical cases are shown in Fig. A.2.5 (a) and (b). We examine only these two cases; all the other cases can be handled similarly.

(a) For region I of Fig. A.2.5 (a), we can consider the polar coordinates as in Fig. A.2.6.

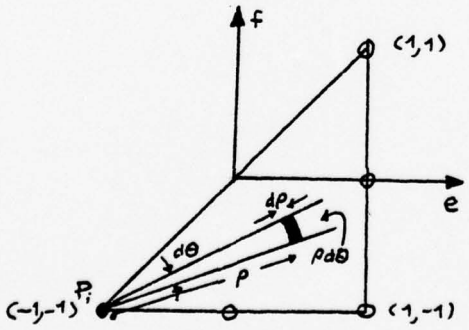

Fig. A.2.6

Thus

$$(\bar{a}_{ij}^{\alpha})_I = -\int_0^{\frac{1}{4}\pi} \int_0^{2\sec\theta} \frac{(N^{\alpha}(e,f) - \delta_{ij}(\alpha)(Dx_{ij}N_1^* + Dy_{ij}N_2^*}{r^2(p_i, q_j(e,f)}$$

$$\frac{+Dz_{ij}N_3^*}{} \, dr \, d\theta$$

where

$$e = r\cos\theta - 1$$

$$f = r\sin\theta - 1$$

and let

$$F_{ij}^{\alpha}(r,\theta) = \frac{-(N(e,f) - \delta_{ij}(\alpha))(Dx_{ij}N_1^* + Dy_{ij}N_2^* + Dz_{ij}N_3^*)}{r_{ij}^2}$$

It is found that

$$\lim_{r\to 0} \bar{F}_{ij}^{\alpha}(r,\theta) = \frac{0}{0}$$

which is indeterminate. However, by using l'Hopital's rule twice we have

$$\lim_{r\to 0} \bar{F}_{ij}^{\alpha}(r,\theta) = \lim_{r\to 0} \frac{-[\,(N^{\alpha}(e,f) - \delta_{ij}(\alpha))(Dx_{ij}N_1^* + Dy_{ij}N_2^* + Dz_{ij}N_3^*]''}{2}$$

where the limit of the numerator part will be some finite number. Therefore, we know that there is no singularity, thus

$$(a_{ij}^{\alpha})_I = \sum_{k=1}^{m1} w_k \sum_{l=1}^{m2} w_l \bar{F}_{ij}^{\alpha}(r_k, \theta_l)$$

where $r \in (0, 2\sec\theta)$ and $\theta \in (o, \frac{1}{4}\pi)$. Similarly, we can conclude that

$$(a_{ij}^{\alpha})_{II} = \sum_{k=1}^{m1} w_k \sum_{l=1}^{m2} w_l \bar{F}_{ij}^{\alpha}(r_k, \theta_l)$$

where $r \in (0, 2\csc\theta)$ and $\theta \in (\frac{1}{4}\pi, \frac{1}{2}\pi)$; so

$$\bar{a}_{ij}^{\alpha} = (\bar{a}_{ij}^{\alpha})_I + (\bar{a}_{ij}^{\alpha})_{II}$$

(b) Similarly, by considering polar coordinates, for region I of Fig. A.2.5 (b), we have

$$(\bar{a}_{ij}^{\alpha})_I = -\int_0^{\tan^{-1}(2)} \int_0^{\sec\theta} \bar{F}_{ij}^{\alpha}(r, \theta)\, dr\, d\theta$$

where $\bar{F}_{ij}^{\alpha}(r, \theta)$ is defined as in (a), but here we have

$$e = r\cos\theta$$

$$f = r\sin\theta - 1$$

Similar to the procedure in (a), we can have

$$(\bar{a}_{ij}^{\alpha})_I = \sum_{k=1}^{m1} w_k \sum_{l=1}^{m2} w_l \bar{F}_{ij}^{\alpha}(r_k, \theta_l)$$

where $r \in (0, \sec\theta)$ and $\theta \in (0, \tan^{-1}(2))$.

Also, we can have $(\bar{a}_{ij}^{\alpha})_{II}$ and $(\bar{a}_{ij}^{\alpha})_{III}$ in the same form, except

$r \in (0, 2\csc\theta)$, $\theta \in (\tan^{-1}(2), \pi - \tan(2))$ for region I

$r \in (0, -\sec\theta)$, $\theta \in (\pi - \tan^{-1}(2), \pi)$ for region II

then we can get

$$\bar{a}^{\alpha}_{ij} = (\bar{a}^{\alpha}_{ij})_I + (\bar{a}^{\alpha}_{ij})_{II} + (\bar{a}^{\alpha}_{ij})_{III}$$

2.2.3 Calculation of b^{α}_{ij}:

$$b^{\alpha}_{ij} = \int_{-1}^{1} \int_{-1}^{1} N^{\alpha}(e,f) \frac{1}{r(p_i, q_j(e,f))} J(e)\, de\, df$$

The two different cases will be

(i) p_i is not situated within j^{th} segment, as shown in Fig. A.2.4. Let

$$H^{\alpha}_{ij}(e,f) = N^{\alpha}(e,f) \frac{1}{r(p_i, q_j(e,f))} J(e)$$

and we thus have

$$b^{\alpha}_{ij} = \sum_{k=1}^{m1} w_k \sum_{l=1}^{m2} w_l H^{\alpha}_{ij}(e_k, f_l)$$

(ii) p_i is situated within j^{th} segment, as shown in Fig. A.2.5. As in 2.2.2, we just consider the typical case, Fig. A.5(a) and (b).

(a) By considering the polar coordinates for region I as shown in Fig. A.2.6 we have

$$(b^{\alpha}_{ij})_I = \int_0^{\frac{1}{4}\pi} \int_0^{2\sec\theta} N^{\alpha}(e,f) J(e,f)\, dr\, d\theta$$

where

$$e = r\cos\theta - 1$$

$$f = r\sin\theta - 1$$

Let

$$H_{ij}^{\alpha}(r,\theta) = N^{\alpha}(e,f)J(e,f)$$

It is obvious that H_{ij}^{α} is free of singularity, therefore

$$(b_{ij}^{\alpha}) = \sum_{k=1}^{m1} w_k \sum_{l=1}^{m2} w_l H_{ij}^{\alpha}(r_k, \theta_l)$$

where $r \in (0, 2\sec\theta)$ and $\theta \in (0, \frac{1}{4}\pi)$.

Similarly, $(b_{ij}^{\alpha})_{II}$ has the same form as $(b_{ij}^{\alpha})_{I}$, except that $r \in (0, 2\csc\theta)$, $\theta \in (\frac{1}{4}\pi, \frac{1}{2}\pi)$, and thus

$$b_{ij}^{\alpha} = (b_{ij}^{\alpha})_{I} + (b_{ij}^{\alpha})_{II}$$

(b) Similar to the procedure described in (a), we have

$$b_{ij}^{\alpha} = (b_{ij}^{\alpha})_{I} + (b_{ij}^{\alpha})_{II} + (b_{ij}^{\alpha})_{III}$$

where $(b_{ij}^{\alpha})_{I}$, $(b_{ij}^{\alpha})_{II}$ and $(b_{ij}^{\alpha})_{III}$ have the same form as shown in (a), except that

$$e = r\cos\theta$$

$$f = r\sin\theta - 1$$

and

$r \in (0, \sec\theta)$, $\theta \in (0, \tan^{-1}(2))$ for region I

$r \in (0, 2\csc\theta)$, $\theta \in (\tan^{-1}(2), \pi - \tan^{-1}(2))$ for region II

$r \in (0, -\sec\theta)$, $\theta \in (\pi - \tan^{-1}(2), \pi)$ for region III

2.2.4 Calculation of k_{1i}^{α} and k_{2j}^{α}:

$$k_{1j}^{\alpha} = \int_{-1}^{1}\int_{-1}^{1} N^{\alpha}(e,f)\ \frac{\partial}{\partial n}\ \frac{1}{r(t,q_j(e,f))} J(e,f)\ de\ df$$

$$k_{2j}^{\alpha} = \int_{-1}^{1}\int_{-1}^{1} N^{\alpha}(e,f)\ \frac{1}{r(t,q_j(e,f))} J(e,f)\ de\ df$$

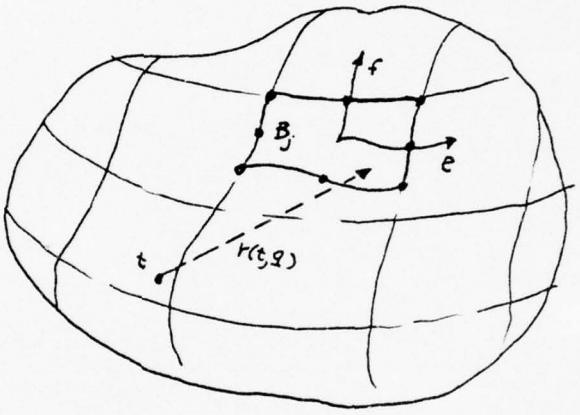

Fig. A.2.7

Since t is an interior point, (cf. Fig. A.2.7) there is no singular case. We can thus calculate k_{1j}^{α}, k_{2j}^{α}, by using (m1 x m2) -point Gaussian quadrature formula, as in those procedures described in A.2.2.2 (i) and A.2.2.3 (i); i.e.

$$k_{1j} = \sum_{k=1}^{m1} w_k \sum_{l=1}^{m2} w_l F_j^{\alpha}(e_k, f_l)$$

$$k_{2j} = \sum_{k=1}^{m1} w_k \sum_{l=1}^{m2} w_l H_j^{\alpha}(e_k, f_l)$$

where

AD-A033 891 KENTUCKY UNIV LEXINGTON DEPT OF ENGINEERING MECHANICS F/G 12/1
THE BOUNDARY INTEGRAL EQUATION METHOD USING VARIOUS APPROXIMATI--ETC(U)
DEC 76 Y S WU AF-AFOSR-2824-75

UNCLASSIFIED AFOSR-TR-76-1313 NL

2 OF 2
ADA033891

END

DATE
FILMED
2 - 77

$$F_j^{\alpha}(e,f) = N^{\alpha}(e,f) \frac{\partial}{\partial n} \frac{1}{r(t,q_j(e,f))} J(e,f)$$

$$H_j^{\alpha}(e,f) = N^{\alpha}(e,f) \frac{1}{r(t,q_j(e,f)} J(e,f)$$

and

$$\frac{\partial}{\partial n} \frac{1}{r(t,q_j(e,f)} J(e,f) = - \frac{1}{r^3(t,q_j(e,f))} [(x_j(q(e,f)) - x(t))n_x +$$

$$(y_j(q(e,f)) - y(t))n_y + (z_j(q(e,f)) - z(t))n_z]$$

APPENDIX III

CALCULATION OF ELEMENTS OF COEFFICIENT MATRIX IN CUBIC SPLINE FUNCTION APPROXIMATION

3.1 Calculation of $\bar{a}_{ij}$:

$$\bar{a}_{ij} = -\int_{B_j} B_2 (s - s_j) \frac{\partial \log r(p_i, q(s))}{\partial n} ds$$

$$- \int_{B_{j+1}} B_1 (s - s_j) \frac{\partial \log r(p_i, q(s))}{\partial n} ds$$

$$- \int_{B_{j-1}} B_2 (s_j - s) \frac{\partial \log r(p_i, q(s))}{\partial n} ds$$

$$- \int_{B_{j-2}} B_1 (s_j - s) \frac{\partial \log r(p_i, q(s))}{\partial n} ds \qquad (3.33)$$

There are various ways to calculate these integrals numerically. One convenient way for the general case which we will illustrate is to adopt the parametric transformation of geometrical coordinates, i.e., to approximate each of the two groups, (B_j, B_{j+1}) and (B_{j-2}, B_{j-1}) in the expression of $\bar{a}_{ij}$, as we did in Chapter 3.1.A. (Consequently we should divide each closed boundary into an even number of intervals to carry out this kind of approximation. See Figures A.3.1 and A.3.2.)

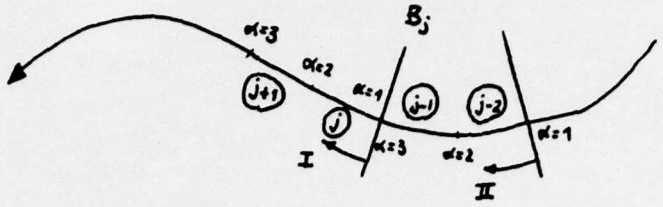

Fig. A.3.1

Taking group $I(B_j, B_{j+1})$ as an example,

$$(\bar{a}_{ij})_I = -\int_{-1}^{0} B_2(s(e) - s_j) \frac{d\theta_{ij}(e)}{de} de$$

$$- \int_{0}^{1} B_1(s(e) - s_j) \frac{d\theta_{ij}(e)}{de} de$$

where

$$B_1(s(e) - s_j) = (2 - \frac{(s(e) - s_j)}{h})^3$$

$$B_2(s(e) - s_j) = (2 - \frac{(s(e) - s_j)}{h})^3 - 4(1 - \frac{(s(e) - s_j)}{h})^3$$

$$s(e) - s_j = \int_{-1}^{e} J(e)de$$

$$= \int_{-1}^{e} \sqrt{(\frac{dN^{\alpha}(e)}{de} x^{\alpha})^2 + (\frac{dN^{\alpha}(e)}{de} y^{\alpha})^2}\, de$$

$$= \Big[\frac{(2ce + b)\sqrt{ce^2 + be + a}}{4c} + \frac{4ac - b^2}{8c\sqrt{c}} \cdot$$

$$x \log(2\sqrt{c(ce^2 + be + a)} + 2ce + b) \Big] - \Big[\frac{(b - 2c)\sqrt{c - b + a}}{4c}$$

$$+ \frac{4ac - b^2}{8c\sqrt{c}} \log(2\sqrt{c(c - b + a)} - 2c + b) \Big]$$

$$a = \tfrac{1}{4}\left[(x^3 - x^1)^2 + (y^3 - y^1)^2 \right]$$

$$b = (x^1 + x^3 - 2x^2)(x^3 - x^1) + (y^1 + y^3 - 2y^2)(y^3 - y^1)$$

$$c = (x^1 + x^3 - 2x^2)^2 + (y^1 + y^3 - 2y^2)^2$$

Then we can calculate $(\bar{a}_{ij})_I$ in the manner shown in A.2.1.1 for both the nonsingular and singular cases. Similarly, we can express $(\bar{a}_{ij})_{II}$ in the same way, except where $s_j - s(e) = \int_e^1 J(e)de$, and

$$\bar{a}_{ij} = (\bar{a}_{ij})_I + (\bar{a}_{ij})_{II}$$

3.2 Calculation of b_{ij}:

$$b_{ij} = -\int_{B_j} B_2(s - s_j)\log r(p_i, q(s))ds$$

$$- \int_{B_{j+1}} B_1(s - s_j)\log r(p_i, q(s))ds$$

$$- \int_{B_{j-1}} B_2(s_j - s)\log r(p_i, q(s))ds$$

$$- \int_{B_{j-2}} B_1(s_j - s)\log r(p_i, q(s))ds \qquad (3.34)$$

Still taking two groups (B_j, B_{j+1}) and (B_{j-2}, B_{j-1}) as in A.3.1 and Fig A.3.1 into consideration, we thus have

$$(b_{ij})_I = -\int_{-1}^{0} B_2(s(e) - s_j)\log r(p_i, q(e))J(e)de$$

$$- \int_0^1 B_1(s(e) - s_j)\log r(p_i, q(e)J(e)de$$

where s(e) - s_j is defined in A.3.1.

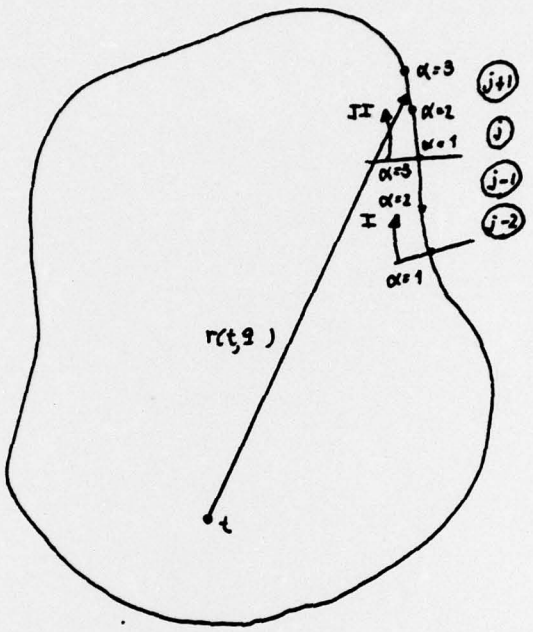

Fig. A.3.2

Without consideration of singular cases, k_{1j} and k_{2j} can be calculated by the same procedures described in A.3.1 and A.3.2 respectively. By using a procedure similar to that described in A.2.1.2, we can calculate $(b_{ij})_I$ for both the nonsingular and singular cases. Then by combination as before, we have

$$b_{ij} = (b_{ij})_I + (b_{ij})_{II}$$

3.3 Calculation of k_{1j} and k_{2j}:

$$k_{1j} = \int_{B_j} B_2 (s - s_j) \frac{\partial \log r(t, q(s))}{\partial n} ds$$

$$+ \int_{B_{j+1}} B_1 (s - s_j) \frac{\partial \log r(t, q(s))}{\partial n} ds$$

$$+ \int_{B_{j-1}} B_2 (s_j - s) \frac{\partial \log r(t, q(s))}{\partial n} ds$$

$$+ \int_{B_{j-2}} B_1 (s_j - s) \frac{\partial \log r(t, q(s))}{\partial n} ds \qquad (3.38)$$

$$k_{2j} = \int_{B_j} B_2 (s - s_j) \log r(t, q(s)) ds$$

$$+ \int_{B_{j+1}} B_1 (s - s_j) \log r(t, q(s)) ds$$

$$+ \int_{B_{j-1}} B_2 (s_j - s) \log r(t, q(s)) ds$$

$$+ \int_{B_{j-2}} B_1 (s_j - s) \log r(t, q(s)) ds \qquad (3.39)$$

ACKNOWLEDGEMENTS

I would like to thank Dr. F. J. Rizzo for his advice and encouragement throughout all phases of my graduate education. I would also like to thank Dr. D. J. Shippy for his valuable assistance during the course of this study.

I would like to thank the Department of Engineering Mechanics of the University of Kentucky for the Research Assistantship it has awarded to me and the support of the present study by the Air Force through Contract AFOSR 75-2824. Also, I gratefully acknowledge the generosity of the University of Kentucky Computing Center for the use of its facilities.

Particular thanks go to Jyawei K. Wu, my wife, for typing the semifinal draft of this thesis.

REFERENCES

[1] Artley, J., Fields and Configurations, Holt, Rinehart and Winston, Inc. (1965).

[2] Hansen, A. G., Similarity Analyses of Boundary Value Problem in Engineering, Prentice-Hall, Inc. (1964).

[3] Kreith, F., Principles of Heat Transfer, 3rd ed. New York, Intext Educational Publishers. (1973)

[4] Forsythe, G. E., and Wasow, W. R., Finite-Difference Methods for Partial Differential Equations. John Wiley & Sons, Inc. (1960).

[5] Strang, G., and Fix, G. J., An analysis of the Finite Element Method, Prentice-Hall, Inc. (1973).

[6] Cruse, T. A., and Rizzo, F. J. ed., Boundary-Integral Equation Method: Computational Applications in Applied Mechanics. ASME AMD. Vol. 11 (1975).

[7] Kellogg, O. D., Foundations of Potential Theory. Dover Publications, Inc. (1964).

[8] Jaswon, M. A., Integral Equation Methods in Potential Theory. I. Proceedings of the Royal Society, Vol. 273, Ser. A. (1963).

[9] Rice, J., The Approximation of Functions, Vol. 1. Addison-Wesley Publishing Company Reading, Mass.

[10] Prenter, P. M., Splines and Variational Methods. John Wiley & Sons, Inc. (1975).

[11] Conte, S. D., and de Boor, C., Elementary Numerical Analysis. 2nd ed. McGraw-Hill, Inc. (1972).

[12] Zienkiewicz, O. C., and Phillips, D. V., An Automatic Mesh Generation Scheme for Plane and Curved Surfaces by Isoparametric Coordinates. Int. J. Numer, Meth. Eng., 3 (1971), pp. 519-528.

[13] Zienkiewicz, O. C., The Finite Element Method in Engineering Science, McGraw-Hill, Inc. (1971).

[14] Ahlberg, J. H., et al: The Theory of Splines and Their Applications. Academic Press (1967).

[15] Greville, T. N. E. ed., Theory and Applications of Spline Function. Academic Press (1969).

[16] Schoenberg, I. J. ed., Approximations with Special Emphasis on Spline Functions. Academic Press (1969).

[17] Schultz, M. H., Spline Analysis. Prentice Hall (1973).

[18] Stroud, A. H., Approximate Calculation of Multiple Integrals. Prentice-Hall, Inc. (1971).

[19] Stroud, A. H., and Secrest, D., Gaussian Quadrature Formulas. Prentice-Hall, Inc. (1966).

[20] Kreyszig, E., Advanced Engineering Mathematics. John Wiley & Sons, Inc. (1967).

[21] Hall, C. A., On Error Bounds for Spline Interpolation. J. Approx. Theory, 1 (1968), pp. 209-218.